2006

# A Novel Type of ZVT-PWM Converter

Xing Gao
*Western University*

# A Novel Type of ZVT-PWM Converter

**By**

**Xing Gao**

Faculty of Engineering
Department of Electrical & Computer Engineering
Graduate Program in Engineering Science

A thesis submitted in partial fulfillment
of the requirements for the degree of
Master of Engineering Science

Faculty of Graduate Studies
The University of Western Ontario
London, Ontario, Canada

THE UNIVERSITY OF WESTERN ONTARIO
FACULTY OF GRADUATE STUDIES

# CERTIFICATE OF EXAMINATION

**Supervisor**

**Dr. Gerry Moschopoulos**

**Supervisory Committee**

**Dr. Lyndon Brown**

**Examiners**

**Dr. Rajiv K. Varma**

**Dr. Michael Naish**

**Dr. Mehrdad Moallem**

**The thesis by**

**Xing Gao**

**entitled:**

## A Novel Type of ZVT-PWM Converter

**is accepted in partial fulfillment of the requirements for the degree of Master of Engineering Science**

**Date**_____

**Chair of the Thesis Examination Board**

# ABSTRACT

High frequency operation of single-switch, pulse width modulated (PWM) converters allows for the reduction of the size and weight of their magnetic and filtering components, but switching losses become significant and must be reduced. The standard approach to minimizing these losses has been to use an active auxiliary circuit that consists of an active switch and passive elements and that is not part of the main power circuit. The auxiliary circuit helps the main power switch turn on with zero-voltage switching (ZVS). The circuit is activated just before the main power switch is to be turned on and is active for only a fraction of the switching cycle, until the switching transition has been completed.

A new type of active auxiliary circuit is presented in this thesis. The main feature of an auxiliary circuit of this new type is that it has the advantages of traditional non-resonant and resonant auxiliary circuits without the disadvantages. In this thesis, the fundamental principles behind the new type of circuit are explained, an example circuit of this type is analyzed, and a design procedure for the selection of the critical components is presented. A variation of the new type of circuit is then discussed, and the feasibility of the new type of auxiliary circuit is confirmed by experimental results obtained from a prototype circuit of a 500W, 100 kHz ZVT PWM boost converter.

**Keywords:** Switch mode power converter, pulse width modulation (PWM), soft-switching, zero-voltage switching (ZVS), efficiency, high-frequency operation.

# ACKNOWLEDGEMENTS

First and foremost, I want to express my sincere gratitude to my supervisor, Dr. Gerry Moschopolous, for his guidance and support during my graduate studies, especially his valuable advice and encouragement to me from the moment I considered starting my Master's program at Western. His practical way of teaching, impressive knowledge, experience, and creative thinking have been a source of inspiration throughout the course and project of my graduate studies.

I am grateful to my other professors for their help. I would like to thank Dr. Rajiv. K. Varma for his support and help with registering a graduate course at University of Waterloo as an OGVS student. I would also like to thank Dr. Wei Wang for his support and encouragement while I was taking his graduate course. The lectures, the long conversations with him, and the guidance he gave me are invaluable.

My work would have not been possible without the help from my family. I would like to express a great amount of gratitude to my wife Yaru Huang and my daughter Weina, for their encouragement and moral support.

Most importantly, I would like to thank my parents and my brothers for everything that they have done for me throughout my life and the joy they have brought to me, just having their support and care. I only hope that what I have accomplished can pay somewhat back for the efforts in raising and making me the person that I am today.

# TABLE OF CONTENTS

**TITLE PAGE**.....i

**CERTIFICATE OF EXAMINATION**.....ii

**ABSTRACT**.....iii

**ACKNOWLEDGEMENTS**.....iv

**TABLE OF CONTENTS**.....v

**LIST OF FIGURES**.....viii

**NOMENCLATURE**.....x

**Chapter 1 Introduction**.....1

1.1 Background Information.....1

1.1.1 Power Electronics System.....1

1.1.2 Single-Switch Converters.....2

1.2 Hard-Switching Converter.....4

1.3 Soft-Switching Converters.....7

1.4 Literature Review.....11

1.5 Thesis Objectives and Outline.....15

**Chapter 2 ZVT Boost Converters with Active Auxiliary Circuits**.....17

2.1 Introduction.....17

2.2 ZVT Boost Converters with Active Auxiliary Circuits.....17

2.2.1 Boost Converter with Non-Resonant Auxiliary Circuit.....19

2.2.2 Boost Converter with Resonant Auxiliary Circuit.....21

2.3 ZVT Boost Converters with Dual Auxiliary Circuits .....23

2.4 Conclusion .....25

**Chapter 3 Analysis of ZVT Boost Converter with a Dual Auxiliary Circuit.....27**

3.1 Introduction .....27

3.2 Operation and Analysis .....27

3.3 Conclusion.....40

**Chapter 4 Converter Design and Auxiliary Circuit Off-Tuning.....41**

4.1 Introduction .....41

4.2 Steady State Characteristic.....41

4.3 Converter Design Procedure .....47

4.3.1 Main Power Circuit Design.....48

4.3.2 Auxiliary Circuit Design.....51

4.4 An Off-Tuned Dual Auxiliary Circuit.....55

4.5 Conclusion.....57

**Chapter 5 Experimental Results.....58**

5.1 Introduction .....58

5.2 Experimental Results and Comparisons.....58

5.3 Conclusion.....66

**Chapter 6 Conclusion.....66**

6.1 Introduction .....66

6.2 Summary .....66

6.3 Conclusion.....68

6.4 Contributions .....69

6.5 Future Work.....69

**References** .....71

**Vita**.....75

# LIST OF FIGURES


1.1 Block Diagram of a Power Electronic System.....2

1.2 Conventional DC/DC boost converter.....3

1.3 Switch voltage and inductor current waveforms for the boost converter.....4

1.4 MOSFET voltage and current waveforms under hard-switching conditions.....5

1.5 Reverse-recovery characteristics of a regular diode and a fast recovery diode.....6

1.6 Typical ZVS resonant boost converter.....8

1.7 ZVT DC/DC boost converter.....9

1.8 Voltage and current waveforms of the ZVT-PWM boost converter.....10

1.9 An improved ZVT-PWM boost converter.....12

1.10 A ZVT-PWM boost converter with magnetic feedback .....12

1.11 ZVT-PWM Converter Proposed in [20].....13

1.12 ZVT-PWM Converter Proposed in [24].....14

1.13 ZVT-PWM Converter Proposed in [25].....15

2.1 Boost Converter with general auxiliary circuit.....18

2.2 Non-resonant auxiliary circuits.....18

2.3 Resonant auxiliary circuits.....19

2.4 PFC boost converter with non-resonant auxiliary circuit .....20

2.5 Typical waveforms of the converter with non-resonance auxiliary circuit.....21

2.6 Boost Converter with Resonant Auxiliary Circuit.....22

2.7 Typical waveforms of the converter with resonance auxiliary circuit.....23

2.8 Derivation of a dual auxiliary circuit.....24

2.9 Dual auxiliary circuits.....25

3.1 (a) A ZVS Boost Converter and (b) A Dual Auxiliary Circuit.....28

3.2 Operation modes of ZVS boos converter.....31

3.3 Typical switching waveforms.....32

4.1 ZVT boost converter with dual auxiliary circuit.....42

4.2 Characteristic curves for $L_{r1}$ =25 μH.....44

4.3 Characteristic curves for $L_{r1}$ =33μH.....45

4.4 Characteristic curves for $L_{r1}$ =40 μH.....46

4.5 Characteristic curves for $L_{r1}$ = 33 μH and K=10 to be used in the selection of $L_{r2}$ .....53

4.6 A ZVT-PWM boost converter with an off-tuned dual auxiliary circuit.....56

5.1 ZVT-PWM boost converter with various auxiliary circuits.....59

5.2 Experimental efficiency comparison at $V_{in}$ = 100V.....60

5.3 Waveforms of $V_{gs2}$ 5V/div and $V_{gs1}$ 5V/div from $S_2$ and $S_1$.....61

5.4 Waveforms of $V_{ds1}$ 100V/div and $V_{gs1}$ 10V/div from $S_1$.....61

5.5 Waveforms of $V_{ds1}$ 100V/div and $I_{s1}$ 1A/div from $S_1$ .....62

5.6 Waveforms of $V_{ds2}$ 100V/div and $V_{gs2}$ 10V/div from $S_2$ .....62

5.7 Waveforms of $V_{gs2}$ 5V/div and $I_{s2}$ 10A/div from $S_2$ .....63

5.8 Waveforms of $V_{gs1}$ 5V/div and $I_{d1}$ 1A/div from $S_1$ and $D_1$ .....63

# NOMENCLATURE

| | |
|---|---|
| AC | Alternating Current |
| BR | Bridge Rectifier |
| EMF | Electromagnetic Force |
| EMI | Electromagnetic Interference |
| EMC | Electromagnetic Compatibility |
| ESR | Equivalent Series Resistor |
| DC | Direct Current |
| LC | Inductor and Capacitor |
| MOSFET | Metal Oxide Semiconductor Field Effect Transistor |
| NRC-ZVS | Non-Resonant-Cell Zero Voltage Switching |
| PFC | Power Factor Correction |
| PWM | Pulse Width Modulation |
| RC-ZVS | Resonant-Cell Zero Voltage Switching |
| RMS | Root mean square |
| SR-PWM | Self-Resonant Pulse Width Modulation |
| SSC | Soft-Switching-Circuit |
| UPS | Uninterruptible Power Supply |
| ZCS | Zero Current Switching |
| ZVS | Zero Voltage Switching |
| ZVT | Zero Voltage Transition |

# Chapter 1 Introduction

## 1.1 Background Information

### 1.1.1. Power Electronics System

Power electronics has applications that span the whole field of electrical power systems from a few Watts to several Megawatts. The main task of power electronics systems is to control and convert electrical power from one form or level to another. Typical power electronics applications include electronic ballasts, high voltage DC systems, power conditioners, UPS systems, power suppliers, motor drives, and electric vehicles. The four main forms of power conversion are:

- AC to DC conversion
- DC to AC conversion
- DC to DC conversion
- AC to AC conversion

Power conversion is mainly performed by the power converter, in which power semiconductor devices are widely used as static switches, for example, diodes, BJTs, MOSFETs and IGBTs. A block diagram of a typical power electronic system is shown in Figure 1.1. The power source may be a DC source or a single-phase/three-phase AC source with line frequency of 50 to 60 Hz or 400Hz; it may be an electric battery, a solar panel, an electric generator or a commercial power supply. The source feeds the input of the power converter, which converts the input power to the required form for a load. The

load may be DC or AC, single-phase or three-phase, and may or may not need transformer isolation from the power source.

The power converter can be an AC/DC converter, a DC/DC converter, a DC/AC inverter or an AC/AC converter depending on the application. Feedback control is used to ensure that the required output voltage and/or current is provided to the load. A goal of power converter technology is to build converters with small size, low weight and low EMI noise and that process substantial power at high efficiency and high power density.

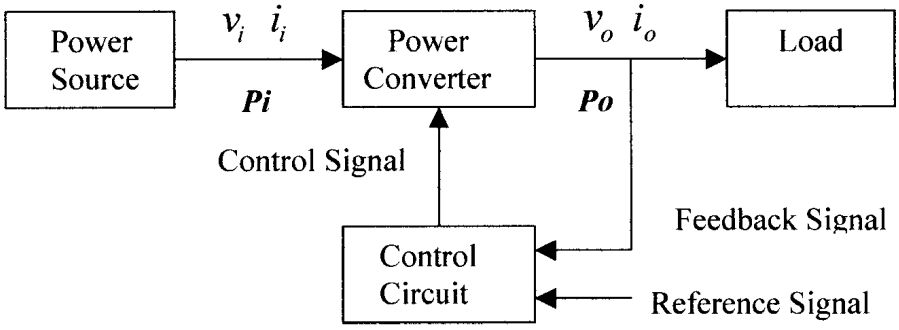


Figure 1.1. Block diagram of a power electronic system.

## 1.1.2. Single-Switch Converters

There are several types of single-switch power converters. The most fundamental single-switch converters are the buck converter, which can step down voltage, the boost converter, which can step up voltage, and the buck-boost converter, which can do both. The buck, boost, and buck-boost converters can be used as DC/DC converters or as AC/DC converters. Most of DC/DC converters are switch-mode converters that operate with active semiconductor devices (i.e., MOSFETs, IGBTs, etc.) functioning as on-off switches. These switches are periodically turned on and off with high switching frequencies ($f_{sw}$ = 20kHz – 1 MHz). The output DC voltage is dependent on the duty

cycle $D$, which is defined as the length of time that a switch is on ($T_{on}$) over the duration of a switching cycle ($T_{sw} = 1/f_{sw}$):

$$D = T_{on}/T_{sw} \quad (1\text{-}1)$$

Figure 1.2 shows a conventional DC/DC boost converter consisting of inductor $L_{in}$, switch S, main diode $D_1$ and output capacitor $C_o$. The converter works as follows:

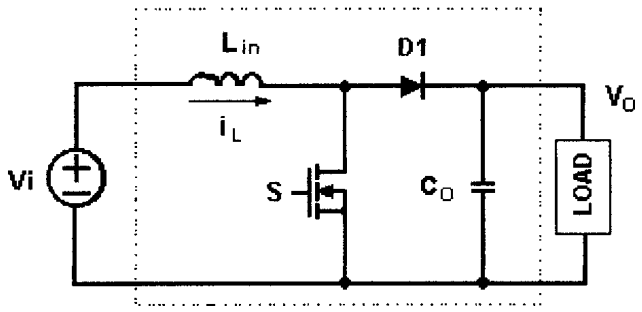


Figure 1.2. Conventional DC/DC boost converter.

When the MOSFET switch S is switched on, current flows from the input source through inductor $L_{in}$ and S and the energy is stored in the inductor. There is no current flowing through diode $D_1$, and the load current is supplied by the energy stored in output capacitor $C_o$. When S is turned off, the energy stored in the inductor $L_{in}$ is transferred to the load as current flows through $D_1$ and the load, recharging $C_o$ as well. Since (1-$D$) is actually the proportion of the switching cycle that S is turned off. The output voltage of a boost converter will always be greater than the input voltage as the ratio of output to input voltage is determined by:

$$V_o/V_i = 1/(1-D) \quad (1\text{-}2)$$

In order to operate the switch S, a pulse train $V_{gs}$ in Figure 1.3 must be applied between the gate and the source of it from a control circuit. The MOSFET is on when the $V_{gs}$ pulse is high and off when it is low. Since the duty cycle of the converter and the

ratio of output to input voltage is determined by the width of the $V_{gs}$ pulses, it is the pulse width that is ultimately used to control and regulate the output voltage. This approach to controlling the output voltage of power converters is called pulse width modulation (PWM).

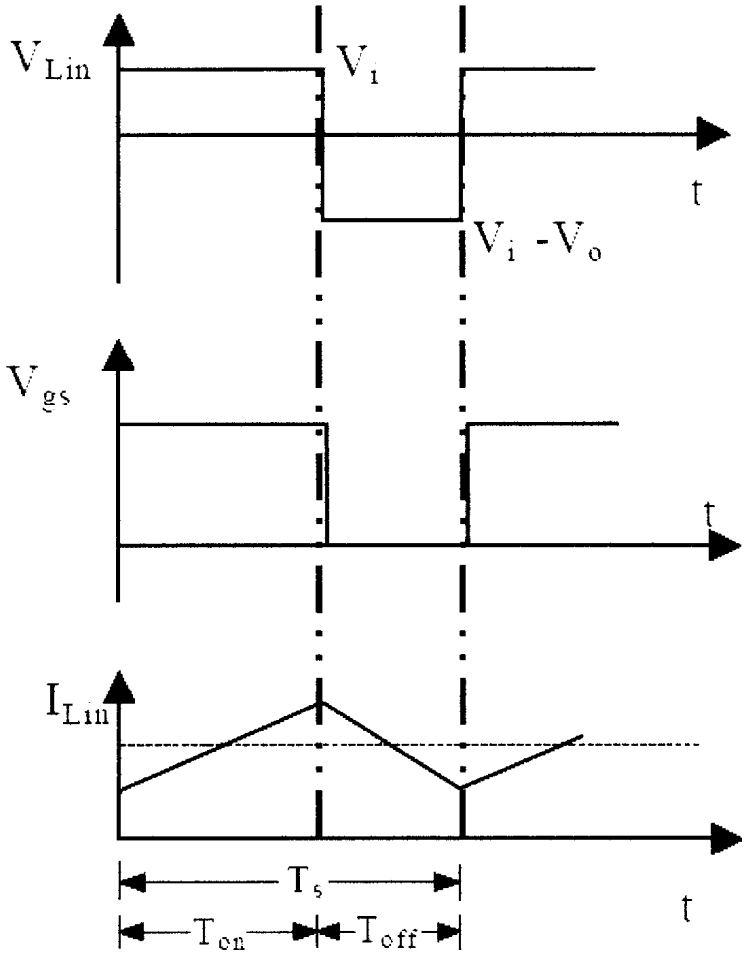


Figure 1.3. Switch voltage and inductor current waveforms for the boost converter.

## 1.2 Hard-Switching Converters

Single-switch PWM power converters are widely used in switched-mode power supplies for computers, telecom, medical, aerospace and other industrial applications.

Most recently, proposed PWM boost converters [11]–[19] have moved to operate with high switching frequency as higher switching frequencies allow for the reduction of magnetic component size, thus increasing power density (W/cm3). Converter operation at high switching frequencies, however, causes higher switching losses and greater electromagnetic interference (EMI). Switching loss mechanisms include power losses caused by the overlap of switch voltage and current during the time interval when the switch is turned on or off and the power loss caused by the dissipation of energy stored in the MOSFETs drain-source when the device is turned on.

The sudden turning on or turning off of a switch is commonly referred to as "hard-switching" in the power electronics literature. Figure 1.4 shows the MOSFET switching voltage and current waveforms under hard-switching conditions. It can be seen that the switching characteristic of the MOSFET has a high dv/dt, a high voltage spike, and significant losses due to voltage and current overlap when the device is turned off. The MOSFET also has a large current spike, a large di/dt and significant losses when the device is turned on.

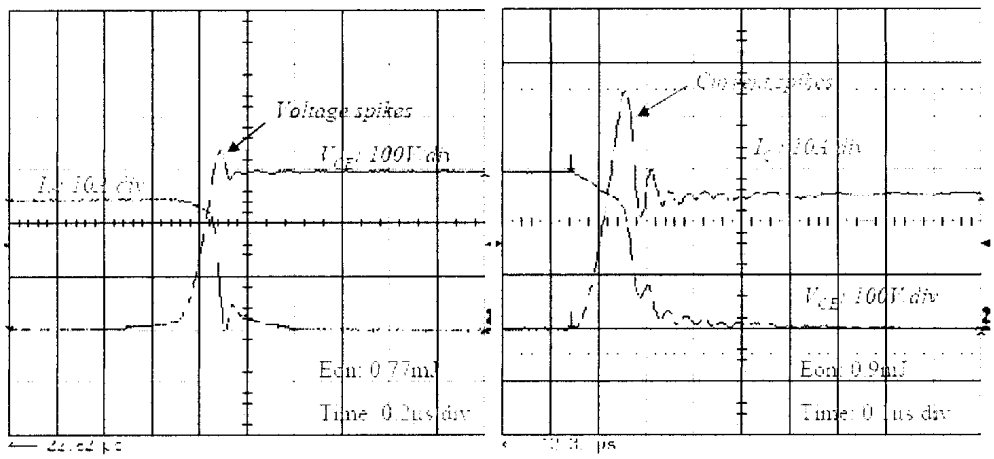


(a) Turn-off (b) Turn-on

Figure 1.4. MOSFET voltage and current waveforms under hard-switching conditions.

Single-switch converters typically have a power diode that can conduct current when the main power switch is off. The current is transferred from the diode to the switch and the diode stops conducting current when the switch is turned on. While the diode stops conducting, there is a duration of time commonly referred to as reverse recovery time, $t_{rr}$, (as shown in Figure 1.5 for a regular diode $t_{RR1}$ and a fast recovery diode $t_{RR2}$) during which there is reverse current flowing through it and reverse voltage across it. Therefore, the conduction losses are generated. This is especially true if the converter switch is operated with hard switching and high frequency because of the abrupt transition of current from switch to diode when the switch is turned on. The reverse-recovery current not only leads to power losses in the diode but also creates electromagnetic interference in the power converter systems that may affect the operation as well performance of other surrounding electrical and electronics equipment. These adverse effects can be significant in high-frequency applications. Fast-recovery diodes with short reverse recovery times ($t_{rr}$) are therefore widely used in high-frequency converters.

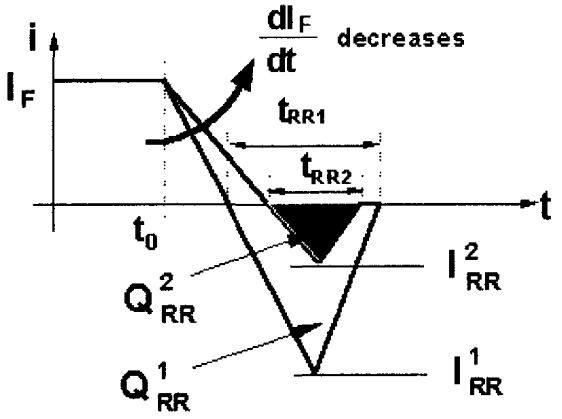


Figure 1.5. Reverse-recovery characteristics of a regular diode and a fast recovery diode.

## 1.3 Soft-Switching Converters

The term "soft-switching" refers to any method of switching where the main power switch in a single-switch converter turns on and/or turns off with a gradual rise or fall of voltage and/or current. The gradual rise and fall of voltage and current can reduce EMI noise and it can also reduce switching losses due to a reduction in the overlap between switch voltage and switch current during a transition. A device operating with soft switching can be made to operate with zero voltage across it or with zero current flowing through it when the device is turned on or off. There are therefore two general types of soft switching: zero-voltage switching (ZVS) and zero-current switching (ZCS). Of the two types, ZVS operation is preferred when using MOSFETs in high switching frequency single-switch converters because it minimizes the power loss due to the discharging of the MOSFETs drain-source capacitance when the device is turned on.

In this section of the chapter, various methods of implementing ZVS in a single-switch converter are discussed.

**1. Resonant Converters with Soft-Switching**

Resonant converters were initially introduced to create an oscillatory voltage or current so that ZVS or ZCS conditions can be achieved for power switches. Figure 1.6 shows a typical ZVS resonant boost converter. The dashed block is the LC resonant auxiliary circuit, which includes resonant components $L_r$ and $C_r$. This LC circuit shapes the switch voltage in such a way that switch S of the boost converter can turn on and off with zero voltage switching.

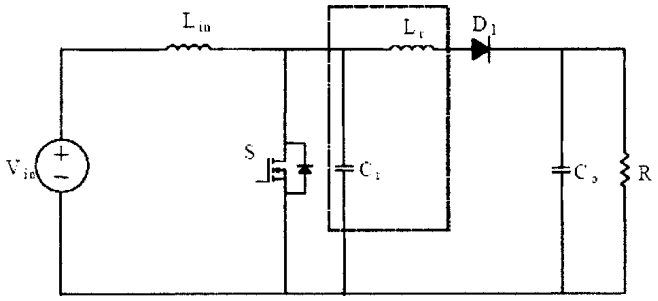


Figure 1.6. Typical ZVS resonant boost converter

Most resonant converters, however, suffer from high peak switch voltage or current stresses in comparison to conventional PWM converters. This leads to higher conduction losses and higher voltage and current rating requirements for the power switches and other circuit components. The other main disadvantage with resonant converters is that when operation over a wide range of input voltage and output load is required, most resonant converters must be made to operate with variable switching frequency control over a wide switching frequency range. This makes it difficult to optimize the design of the ZVS converter.

**2. PWM converters with soft - switching**

The most popular approach to implementing ZVS in single-switch converters is the use of resonant-transition techniques. Resonant-transition soft-switched converters combine the advantages of conventional fixed switched frequency PWM converters and resonant converters and have been developed to overcome the disadvantages of resonant converters. These can be zero-voltage transition (ZVT) converters or zero-current transition (ZCT) converters.

A number of zero-voltage-transition boost converters [1]–[17] have been proposed in recent years, including the one shown in Figure 1.7. All of these converters have an auxiliary circuit that is added to the main boost converter and used to ensure that the boost diode has a soft turn off and that the boost switch is turned on with zero-voltage switching (ZVS). The auxiliary circuit consists of a switch and passive snubber circuit.

The operation of the auxiliary circuit occurs only during the turn-on and turn-off of the main converter switch with a very small portion of switching cycle. Since the auxiliary circuit is only activated for a small portion of the switching cycle, the circuit behaves almost like a conventional PWM converter, but with smoother voltage and current transition. The components in the auxiliary circuit handle a fraction of the power compared to those in the main power circuit and thus lower rated components can be used. This is especially true of the auxiliary switch, which can be a device smaller than that of the main power switch and therefore operate with less switching losses. It is this difference in switching losses that causes the overall efficiency of the converter to be improved.

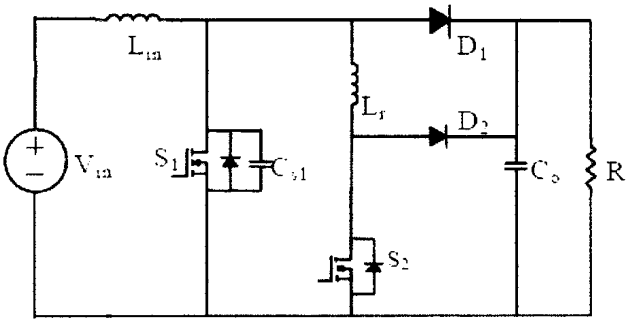


Figure 1.7. ZVT DC/DC boost converter

Comparing Figure 1.7 with Figure 1.2, it can be seen that ZVT converter is identical to the conventional boost converter except that an auxiliary circuit is added to help the

main switch $S_1$ turn-on with ZVS. This auxiliary circuit consists of an inductor $L_r$, a diode $D_2$ and an auxiliary switch $S_2$. Capacitor $C_{s1}$ represents the total capacitance across $S_1$, which consists of the MOSFET's internal output capacitance and an external capacitance cross the drain and source of $S_1$. $C_{s1}$ delays the voltage rise across the switch so that $S_1$ can be turned off with ZVS. Assuming that the inductance of input inductor $L_{in}$ and the capacitance of output capacitor $C_o$ are large enough to maintain the input current $I_{in}$ and the output voltage $V_o$ constant during a switching cycle for the purpose of simplicity, the converter's operation can be explained in the following manner with typical waveforms shown in Figure 1.8.

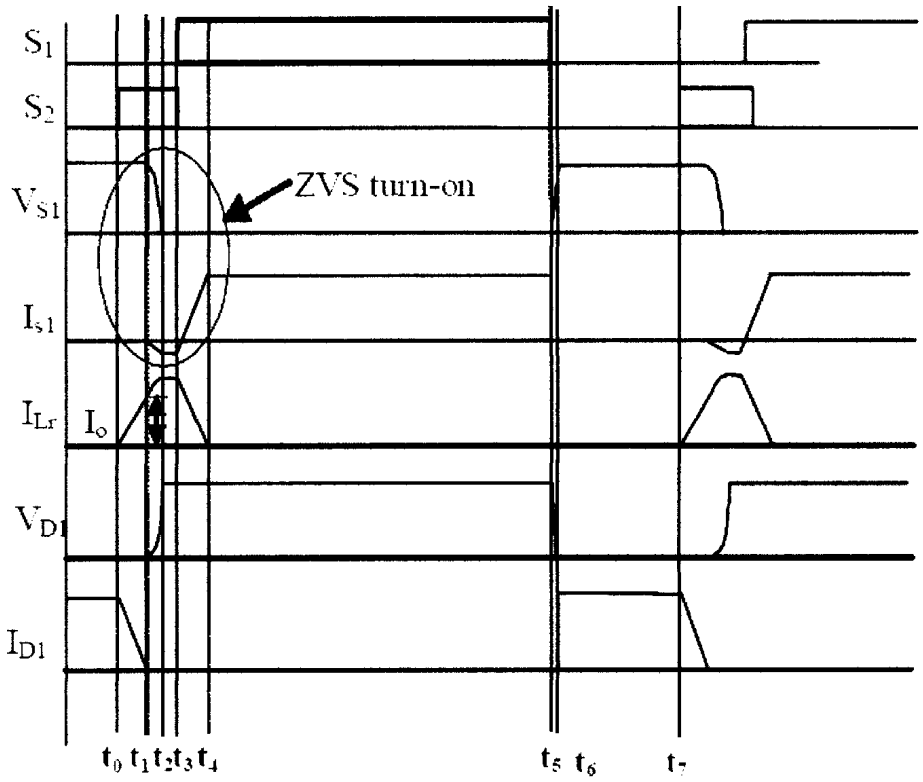


Figure 1.8. Voltage and current waveforms of the ZVT-PWM boost converter.

The converter works exactly like a conventional PWM boost converter until just before the main switch $S_1$ is to be turned on. When the auxiliary switch turns on, the

current through $L_{r1}$ ramps up linearly until it reaches the same level as the input current $I_{in}$. At that moment, the current previously flowing through $D_1$ has been completely diverted to the auxiliary circuit. If the rate of current transfer from $D_1$ to the auxiliary circuit has been sufficiently gradual, then $D_1$ will have little or no reverse recovery current. When current ceases to flow through $D_1$, the voltage across $C_{s1}$ is no longer clamped to the output voltage and $C_{s1}$ begins to discharge into the auxiliary circuit. The current flowing through $L_{r1}$ continues to rise as the voltage across $C_{s1}$ drops until $C_{s1}$ has been completely discharged and the voltage across it is zero.

Since the current flowing in the auxiliary circuit is greater than the input current and $C_{s1}$ has been discharged, the difference in the two currents begins to flow through the anti-parallel body diode of $S_1$. Since the voltage across $S_1$is clamped to zero when this happens ($t = t_2$ in Fig. 1.8), the switch can be turned on with ZVS. When the auxiliary switch $S_2$ is turned off, all the energy stored in $L_{r1}$ is transferred to output through $D_2$ until the current flowing through this inductor is zero; the operation of the converter then becomes identical to that of conventional boost converter. When $S_1$ is turned off, $V_{Cs1}$, the voltage across $S_1$, rises until it is equal to the output voltage $V_o$, $D_1$ then conducts and continues to do so until the start of the next switching cycle.

## 1.4 Literature review

A number of auxiliary circuits for single-switch ZVT-PWM converters have been proposed in recent years [11]–[30], with the auxiliary circuit shown in Figure 1.7 being one of the first and simplest ones [11]. Although this converter can operate with a higher efficiency than conventional PWM Boost converters, the auxiliary switch must operate

with a hard turn-off, which creates significant power losses and generates EMI noise. Other auxiliary circuits have therefore been proposed to overcome the deficiencies of this circuit.

The auxiliary circuit proposed in [13] used an additional snubber circuit to "snub" or to limit the peak voltage across the auxiliary switch when it is turned off. The circuit proposed in [15] was a variation of the one proposed in [13] that allowed the auxiliary switch to turn off with ZVS by adding an extra capacitor. Likewise, the auxiliary circuit proposed in [16], shown in Figure 1.9, is similar to the circuit proposed in [11], but the auxiliary switch can turn off with ZVS due to the addition of a capacitor $C_r$. Other circuits based on the one proposed in [11] have been proposed in [17] – [20].

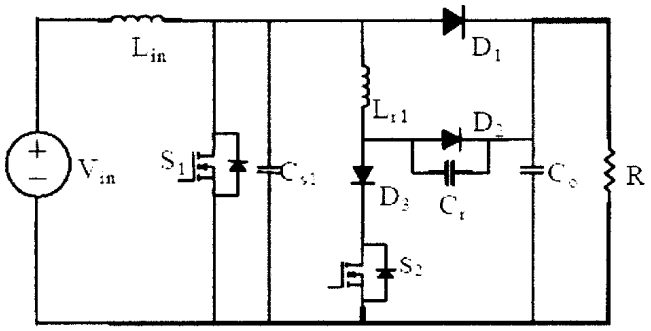


Figure 1.9. An improved ZVT-PWM boost converter.

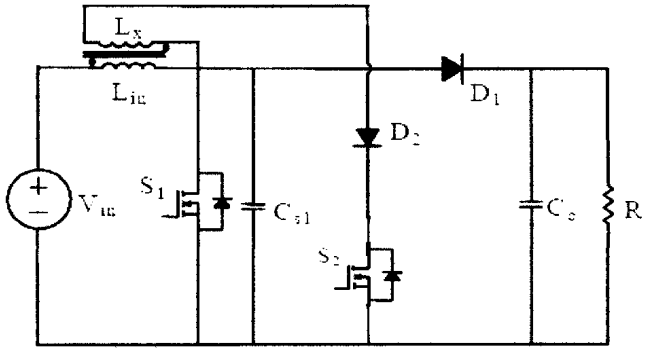


Figure 1.10. A ZVT-PWM boost converter with magnetic feedback.

The introduction of a coupled inductor or transformer in the auxiliary circuit to reduce the effects of the hard turn-off of the auxiliary switch in the converter proposed in [11] was proposed in [21] and shown in Figure 1.10.

The input inductor of the converter is coupled to the auxiliary circuit inductor so that it acts like a current transformer during the time when the auxiliary circuit is active. It provides an alternative current path so that not all of the current originally flowing through diode $D_1$ flows in the auxiliary circuit after the auxiliary switch is turned on. As a result, the turn-off of the auxiliary switch is much less harder since the less current must be interrupted. The main disadvantage of this auxiliary circuit is the input current has a sharp negative peak during the transition period, which increases EMI. Improvements to this circuit were proposed in [22] but the design of the auxiliary circuit transformer is very complicated and extra conduction losses are introduced.

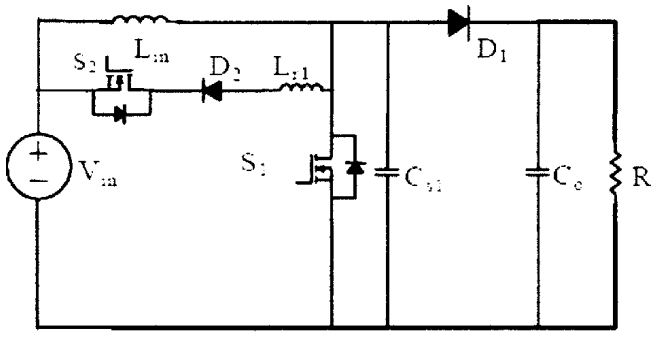


Figure 1.11. ZVT-PWM boost converter proposed in [20].

A different type of auxiliary circuit, not based on the one proposed in [11], was proposed in [20] and shown in Figure 1.11. This circuit transfers the energy stored in inductor $L_{r1}$ of the auxiliary circuit to the input; it is very simple and the auxiliary switch $S_2$ can be turned off with ZCS. The drawbacks of this circuit are that it needs a floating

gate drive circuit for $S_2$ that might be difficult to implement and it can only be implemented in converters that operate with an output voltage at least twice as large as the input voltage.

Most of the auxiliary circuits that have been reviewed so far in this section are considered to be non resonant as these circuits must interrupt current when they are turned off. In order to achieve a soft, turn-off of the auxiliary switch to decrease EMI noise and increase efficiency, resonant auxiliary circuits were proposed, such as the ones proposed in [24], [25] and shown in Figure 1.12 and Figure 1.13 respectively.

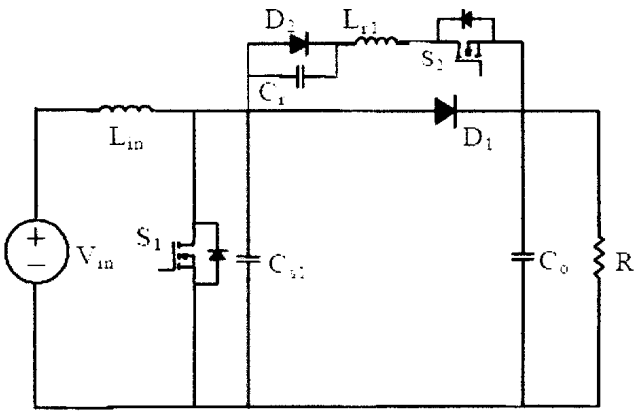


Figure 1.12. ZVT-PWM boost converter proposed in [24].

Resonant auxiliary circuits have a resonant circuit consisting of a capacitor in series with an inductor that can force negative current to flow through the anti-parallel diode of the auxiliary switch; the negative current allows the auxiliary switch to turn off with ZVS. This negative current, however, must circulate in the auxiliary circuit for some length of time and must also flow through the main switch. This leads to an increase in conduction losses and additional peak current stress in the main switch. Other resonant

auxiliary circuits that try to reduce the amount of negative circulating current and do not require a floating gate drive for the auxiliary switch have been proposed in [28].

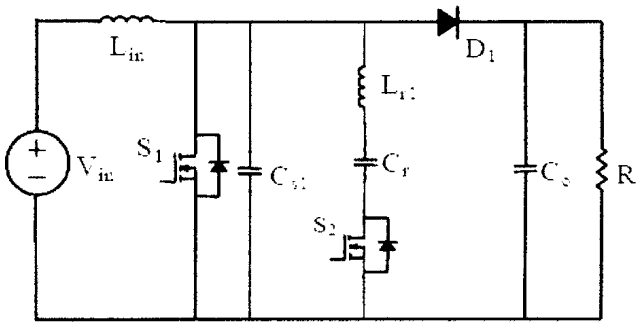


Figure 1.13. ZVT-PWM boost converter proposed in [25].

## 1.5 Thesis Objectives and Outline

The main objectives of this thesis are (i) to propose a new type of auxiliary circuit that can be used in ZVT-PWM converters that combine the advantages of the non-resonant and resonant types of auxiliary circuits, and (ii) to study, characterize and examine the properties and characteristics of this new type of circuit through mathematical analysis and experimental work. The thesis is organized as follows:

Chapter 2 describes the operation of a ZVT-PWM boost converter. Both non-resonant and resonant active auxiliary circuits are presented, their operation is explained, and examples of each type are discussed. A new type of dual active auxiliary circuit that combine the benefits of the non-resonant and the resonant auxiliary circuit is derived. The derivation of a circuit belonging to the new type of converter is also presented.

Chapter 3 describes the operation of an example converter using the new type of dual auxiliary circuit presented in Chapter 2. The different modes of operation during a

switching cycle are explained, and a mathematical analysis of each mode is provided. The results of the analysis are used to examine the steady-state characteristics of the converter in Chapter 4.

In Chapter 4, the steady-state characteristics of the converter discussed in Chapter 3 are examined and are used as part of a design procedure that can be used to select appropriate values for converter critical components. The procedure is demonstrated with an example and can be used to design other ZVT boost converters with dual auxiliary circuits. Also in Chapter 4, a variation of the converter obtained from Chapter 3 is presented and its various modes of operation are discussed.

In Chapter 5, experimental results from an experimental prototype of 500W, 100 kHz ZVT-PWM boost converter are presented. The prototype was implemented with the new type of dual auxiliary circuit presented in Chapter 3, the variation presented in Chapter 4, the original non-resonant auxiliary circuit and resonant auxiliary circuit separately to compare the efficiency performance. The efficiency of the converter operating with each of these four circuits is shown and conclusions about these circuits are made.

Chapter 6 presents the summaries and contributions of this thesis as well as suggestions for future work.

# Chapter 2 ZVT Boost Converters With Active Auxiliary Circuits

## 2.1 Introduction

This chapter will discuss the operation of active auxiliary circuits that allow the main power switch in PWM boost converters to operate with soft-switching, thus reducing power losses, component stresses, and EMI noise. In this chapter, two types of active auxiliary circuits are discussed, their advantages and disadvantages are explained, and examples of each type are presented. Based on these two types of circuits, a new family of active auxiliary circuits can be generated. The derivation of a circuit belonging to the new family will be introduced and other circuits of the same family are also presented.

## 2.2 ZVT Boost Converters with Active Auxiliary Circuits

Most ZVT-PWM converters have an active auxiliary circuit parallel to the main component intending to achieve soft-switching transitions for the main power switch. In a boost converter, the auxiliary circuit usually is connected to the main circuit as showed in Fig. 2.1. The auxiliary circuit basically has three connecting points (a, b and c) although some circuits may not have point c, as indicated by the dashed line shown in Fig. 2.1. This auxiliary circuit has the following advantages: 1) The current through the auxiliary circuit depends on the output voltage and the duty cycle of gate signal at the auxiliary

switch, 2) this current is unrelated to input voltage, and 3) the auxiliary switch can have a gating signal that is referenced to ground.

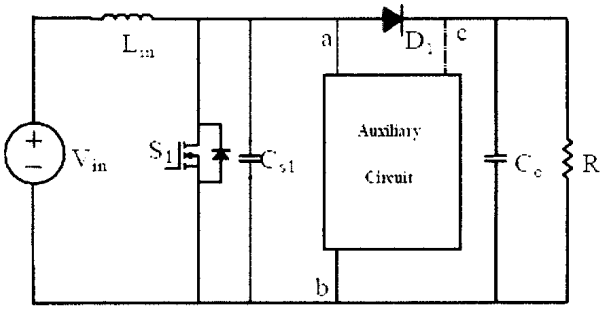


Fig. 2.1. Boost converter with general auxiliary circuit.

Fig. 2.2 and Fig. 2.3 show the two basic types of auxiliary circuits. The circuits in Fig. 2.2 are considered to be non-resonant auxiliary circuits because the current is interrupted when the auxiliary switch is turned off. The circuits in Fig 2.3 are considered to be resonant auxiliary circuits because the LC components in the circuit shape the auxiliary switch current so that zero current occurs when the switch is turned off. The auxiliary circuits shown in Fig. 2.2 (b)-(d) are derivations of the non-resonant circuit Fig. 2.2(a), and those shown in Fig. 2.3 (b)-(d) are derivations from the resonant circuit Fig. 2.3(a).

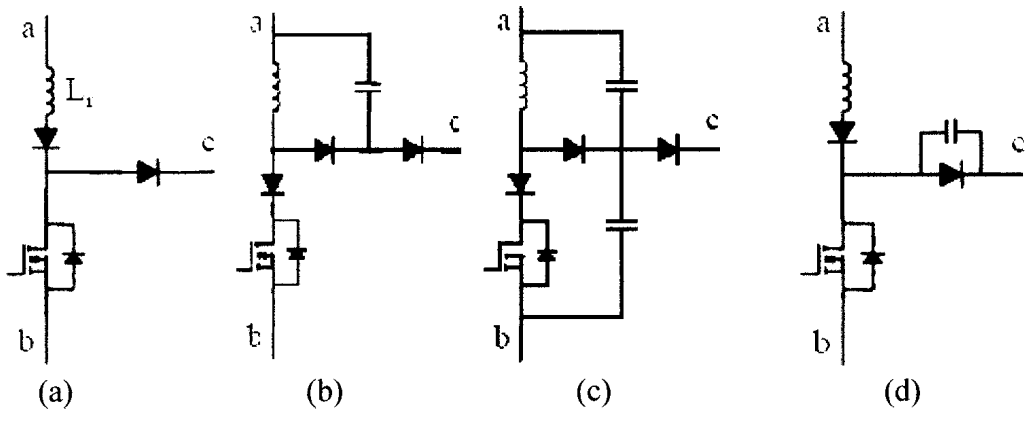


Fig. 2.2. Non-resonant auxiliary circuit.

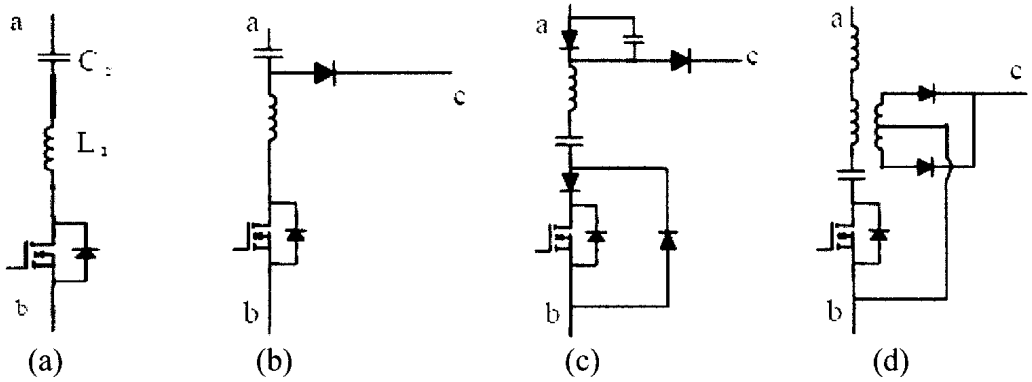


Fig. 2.3. Resonant auxiliary circuits.

### 2.2.1 Boost Converter with Non-Resonant Auxiliary Circuit

In order to explain how a PWM boost converter with a non-resonant auxiliary circuit operates, the operation of an example converter will be discuss in this section. A ZVT PWM boost converter using the non-resonant auxiliary circuit shown in Fig. 2.2 (b) is shown in Fig. 2.4, and its waveforms are shown in Fig. 2.5. Its operation is very similar to that of the conventional ZVT boost converter (Fig. 1.7) except for the $S_2$ turn-off and the $S_1$ turn-off. The converter operates under the assumption that the $L_{in}$ and $C_o$ are large enough to be considered as a constant current source and a constant voltage source. Its operations are discussed in following modes:

The turn on of the main switch $S_1$ is preceded by the conducting of the auxiliary $S_2$ at $t = t_0$. Before that, both $S_1$ and $S_2$ are off and the source current is flowing to the load through $D_1$. The ZVT PWM boost converter is working as a conventional PWM converter. The current through the non-resonant inductor $L_r$ and the voltage across capacitor $C_1$ are initially zero before the switching cycle begins at $t = t_0$.

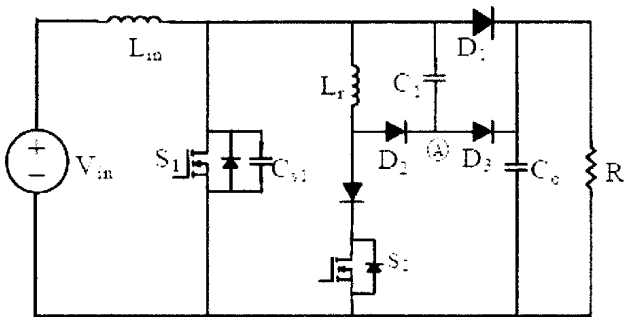


Fig. 2.4. PWM boost converter with non-resonant auxiliary circuit.

Mode 1 [$t_0$-$t_1$]: At $t = t_0$, the auxiliary switch $S_2$ is turned on and the current through $L_r$ builds up linearly reaching first the level of the main inductor current $I_o$, and then causing the diode current to reverse. The peak reverse current $I_{DR}$ of the main diode D depends on the forward current value and the downward slope.

Mode 2 [$t_1$-$t_2$]: Abruptly at $t = t_1$, $D_1$ recovers its blocking characteristics and no longer conducts any current and capacitor $C_{s1}$ begins to discharge as the voltage across it is now not clamped to the output voltage. So the current through $L_r$ continues rising until $C_{s1}$ is totally discharged when $t = t_2$.

Mode 3 [$t_2$-$t_3$]: At $t = t_2$, the voltage cross the $C_{s1}$ almost zero and the body diode of $S_1$ conducts current through the auxiliary circuit. Therefore, $S_1$ can be turned on with ZVS sometime during this interval.

Mode 4 [$t_3$-$t_4$]: When $S_2$ is turned off at $t = t_3$, the current through $L_r$ is diverted to $D_2$ and charges capacitor $C_1$. This interval ends when the current through $L_r$ is zero.

Mode 5 [$t_4$-$t_5$]: The converter operates like a conventional PFC boost converter during this interval.

Mode 6 [$t_5$-$t_6$]: $S_1$ is turned off at $t = t_5$. Capacitor $C_{s1}$ is charged until $D_3$ begins to conduct at $t = t_6$.

Mode 7 [$t_6$-$t_7$]: $C_1$ is discharged during this interval through $D_3$. This interval ends when $C_1$ is totally discharged. The next cycle begins after $t = t_7$.

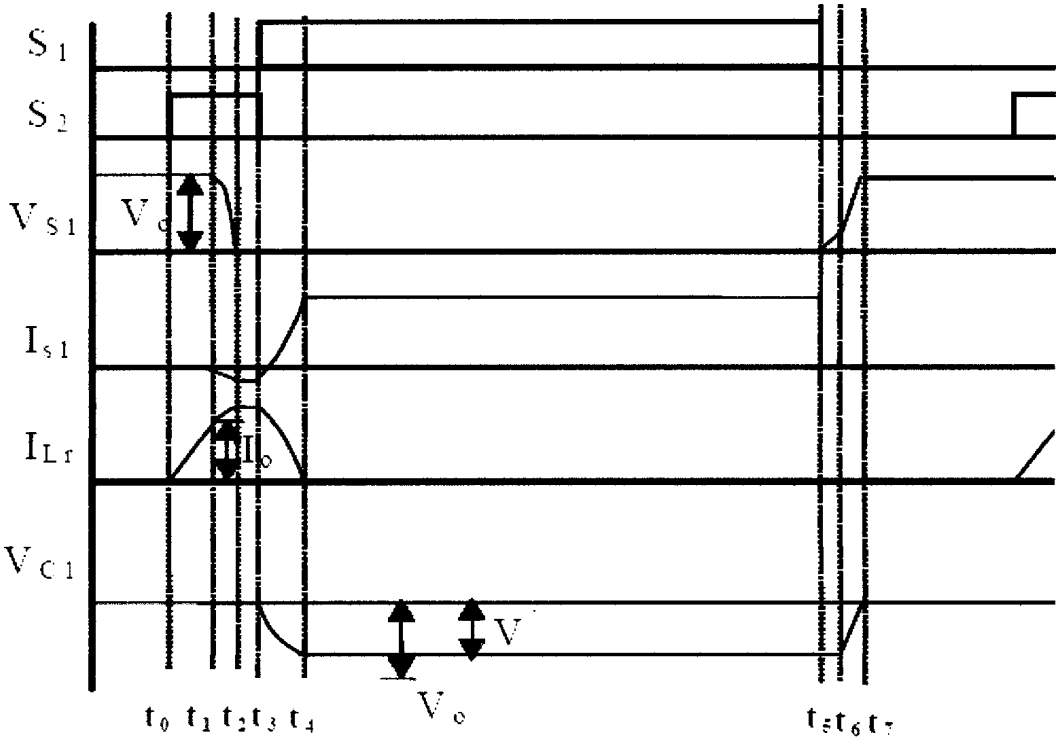


Fig. 2.5. Typical waveforms of the converter with non-resonance auxiliary circuit.

## 2.2.2 Boost Converter with Resonant Auxiliary Circuit

To illustrate how a ZVT PWM boost converter with a resonant auxiliary circuit operates, the operation of an example converter will be discussed in this section. Fig. 2.6 is a ZVS boost converter using the resonant auxiliary circuit shown in Fig. 2.3(a), and its waveforms are shown in Fig. 2.7. The converter operates in the following manner:

Mode 0 [$t<t_0$]: Both switches $S_1$ and $S_2$ are off, the current in the main inductor $L_{in}$ is flowing through $D_1$ to the load and output capacitor $C_o$. Also there is the negative value of voltage $V_{Cr}$ across capacitor $C_r$.

Mode 1 [$t_0$-$t_1$]: At t = $t_0$, the auxiliary switch $S_2$ is turned on and current in the auxiliary circuit rises up linearly.

Mode 2 [$t_1$-$t_2$]: The current through diode $D_1$ stops flowing. $C_{s1}$ begins to discharge the voltage $V_{Cs1}$ across and it is now not clamped to the output voltage. $C_{s1}$ is totally discharged when t = $t_2$.

Mode 3 [$t_2$-$t_3$]: The anti-parallel body diode of $S_1$ conducts and $S_1$ is turned on with ZVS sometime during this interval.

Mode 4 [$t_3$-$t_4$]: The current continues to flow in the auxiliary circuit. Sometime during this interval, $I_{Lr}$ becomes negative due to the resonant interaction between $L_r$ and $C_r$. The current from the auxiliary circuit then flows in $S_1$.The anti-parallel diode of the auxiliary switch $S_2$ then conducts, and $S_2$ can be turned off with ZVS.

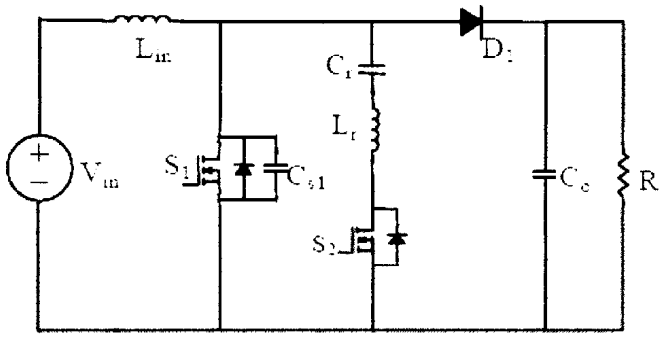


Fig. 2.6. Boost Converter with Resonant Auxiliary Circuit.

Mode 5 [$t_4$-$t_5$]: Negative current continues to flow in the auxiliary during this interval. At t = $t_5$, $I_{Lr}$ becomes zero and $V_{Cr}$ is negatively charged.

Mode 6 [$t_5$-$t_6$]: The converter operates as a conventional PWM boost converter during this interval.

Mode 7 [$t_6$-$t_7$]: Switch $S_1$ is turned off and $C_{S1}$ is charged until $V_{Cs1}$ is equal to the output voltage.

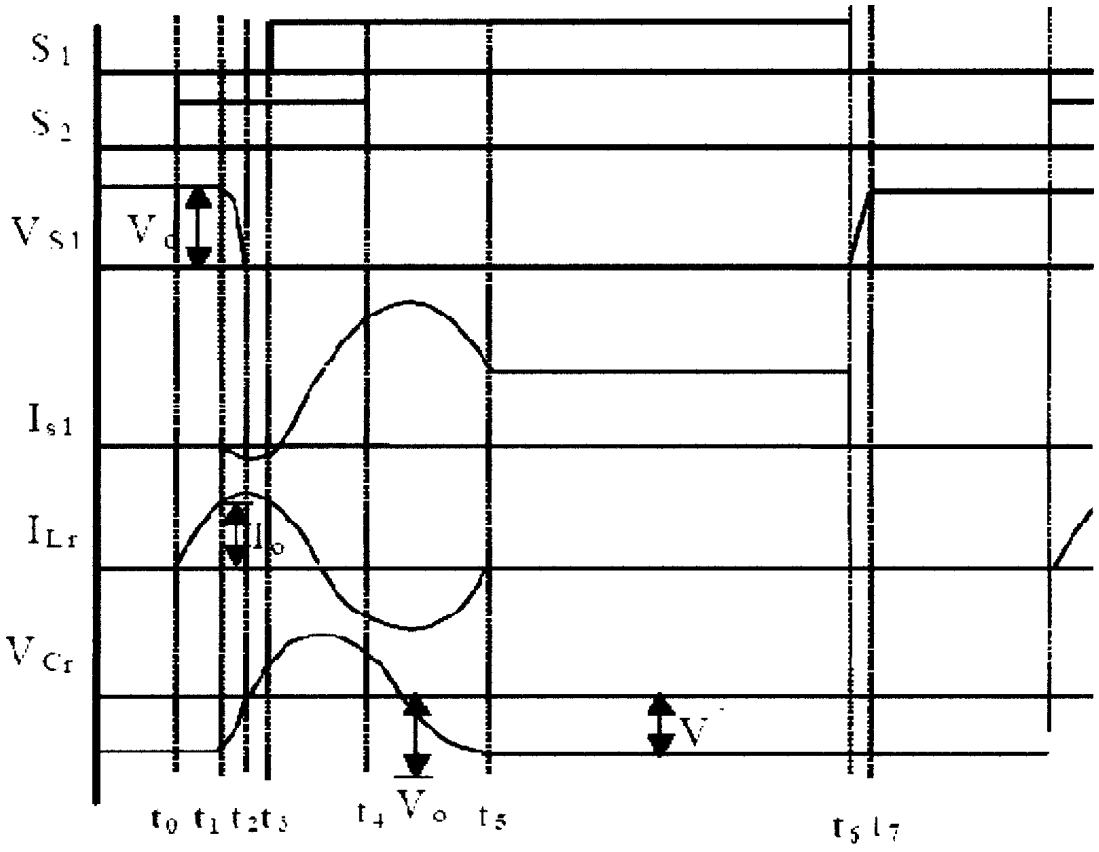


Fig. 2.7. Typical waveforms of the converter with resonance auxiliary circuit.

## 2.3 ZVT Boost Converters with Dual Auxiliary Circuits

ZVT boost converters with non-resonant auxiliary circuits and ZVT-PWM converters with resonant auxiliary circuits have their respective advantages and disadvantages. In converters with non-resonant auxiliary circuits, there is no added current stress in the main switch because no negative current flows through the auxiliary switch, but the auxiliary switch has a hard turn-off that results in switching losses and the generation of

EMI noise. In converters with resonant auxiliary circuits, current through the auxiliary switch can naturally become negative, which enables the auxiliary switch to be turned off with ZVS, but the main switch has added current stress due to the negative current through the auxiliary circuit. To combine the advantages of these two types of converters while minimizing the disadvantages, a new family of dual auxiliary circuits for ZVT-PWM converters is proposed in this thesis. It is possible to derive new dual auxiliary circuit cells in ZVT PFC boost converters that combine the advantages of resonant and non-resonant cells while minimizing the disadvantages of each type. Fig 2.8 shows an example of how a proposed converter can be systematically formed by combining a non-

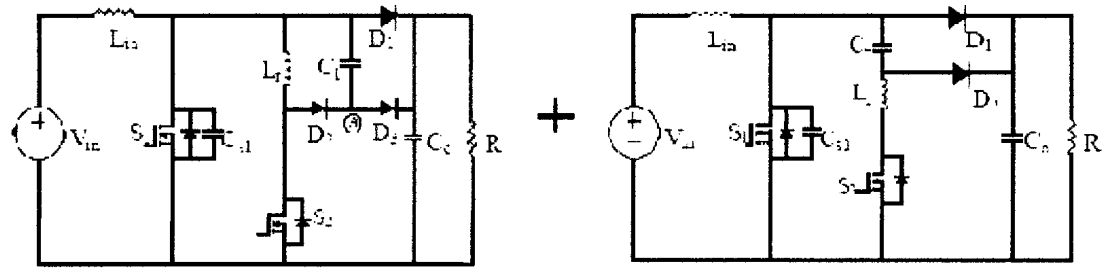

(a) Boost converter with non-resonant auxiliary circuit (b) Boost converter with resonant auxiliary circuit

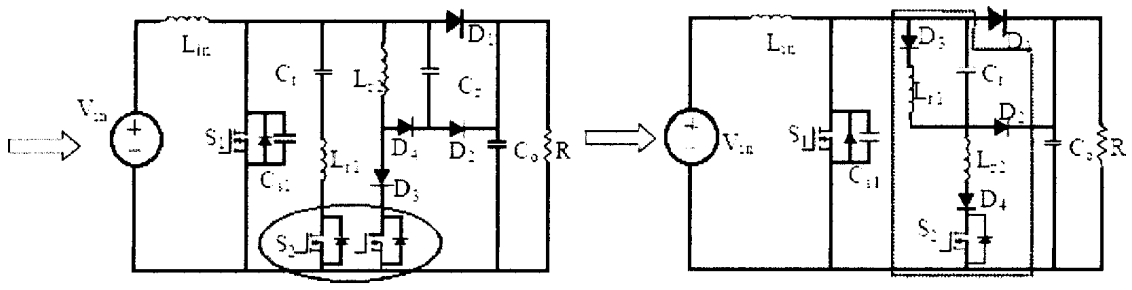

(c) Combination circuit (d) Boost converter with dual auxiliary

Fig. 2.8. Derivation of a dual auxiliary circuit.

resonant cell with a resonant cell. This involves connecting both resonant and non-resonant branches to a single switch and eliminating the other switch, placing a common inductor in series with the switch.

Note that the final dual cell has two resonant branches: a non-resonant branch consisting components: $L_{r1}$, $D_2$, $D_3$, $D_4$ and a resonant branch consisting of components: $L_{r2}$, $C_r$ $D_4$. The function of capacitor $C_1$ in the non-resonant cell shown in Fig. 2.8(a) is performed by the resonant branch capacitor $C_r$. Energy from non-resonant branch $L_r$ is transferred to $C_r$, which is then eventually transferred to the output.

Fig 2.9 shows several other dual auxiliary circuits that have been created by combining non-resonant and resonant auxiliary circuits. Each PWM dc-dc converter with a dual auxiliary circuit in Fig. 2.9 can operate with a ZVS turn-on and turn-off of the main switch and a ZCS turn-on and turn-off of the auxiliary switch, without additional current stresses on the main switch.

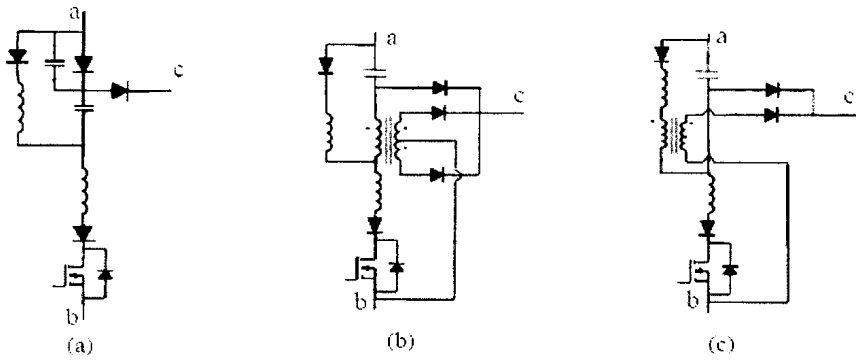


Fig. 2.9 Dual auxiliary circuits

## 2.4. Conclusion

A novel type of active auxiliary circuits that can be used to achieve soft-switching operation for the main power switch and auxiliary switch in PWM boost converters were

presented. Each circuit in this new family can be derived by combining a non-resonant auxiliary circuit with a resonant auxiliary circuit. Such a dual circuit can operate with soft switching for the auxiliary switch as is the case with a resonant auxiliary circuit, without additional current stresses, as is the case for a non-resonant circuit. In this chapter, the operation of a boost converter with example non-resonant and resonant auxiliary circuits was presented, and the derivation of an example dual auxiliary circuit was shown. The configuration of a proposed PWM boost converter with dual auxiliary circuit is presented.

# Chapter 3 Analysis of ZVT Boost Converter With a Dual Auxiliary Circuit

## 3.1 Introduction

In this chapter, the operation of a ZVT-PWM boost converter with a dual active auxiliary circuit is discussed in detail. The modes of operation that the converter goes through during a switching cycle are explained, and a mathematical analysis for each mode is performed. The results of the analysis will be used to examine the steady-state characteristics of the converter in the next chapter.

## 3.2 Operation and Analysis

Figure 3.1 (a) is the ZVT boost converter with an active auxiliary circuit obtained from Chapter 2. In this circuit configuration, $S_1$ is the main power switch that allows energy to be transferred to inductor $L_{in}$ when it is turned on. Then the energy stored in $L_{in}$ is transferred to the output bus when $S_1$ is turned off. Output capacitor $C_o$ acts as a filter to smooth out the ripple of the output voltage so that a regulated DC voltage is fed to the load R. Figure 3.1(b) shows the active auxiliary circuit that was formed by combining a non-resonant cell with a resonant cell and an auxiliary switch in the previous chapter. It consists of inductors $L_{r1}$, $L_{r2}$, diodes $D_2$, $D_3$, $D_4$, capacitor $C_r$ and switch $S_2$. In this section, the all modes of the steady-state converter operation are explained and a

mathematical analysis of each mode of operation is given. The equations that characterize each mode of auxiliary circuit operation described in this section.

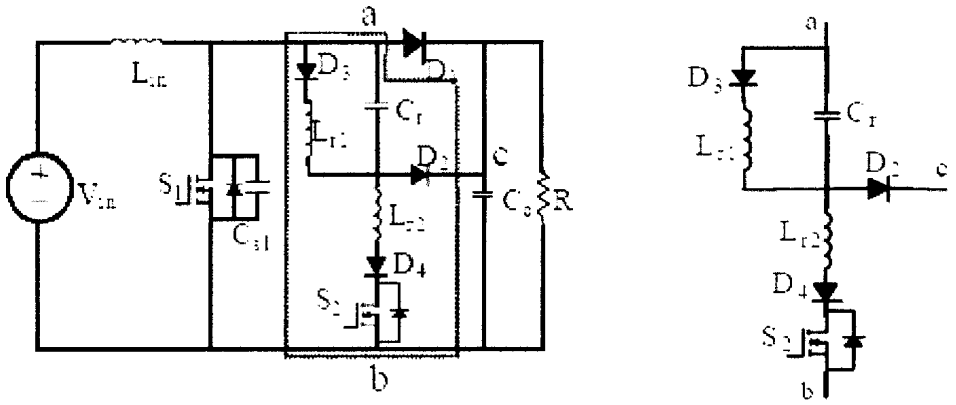


Figure 3.1. (a) A ZVT boost converter and (b) A dual auxiliary circuit.

It should be noted that only the key equations for the specific operating intervals of auxiliary circuit are presented because the proposed converter behaves like a conventional PWM boost converter during most of the switching cycle. The equations have been derived using the following assumptions:

(i) The input inductor is large enough to be considered as a constant DC current source during the time that current is flowing through the auxiliary circuit.

(ii) The output filter capacitor is large enough to be considered as a voltage source during the switching cycle.

(iii) The auxiliary switch has a resistance when it is turned on.

(iv) All inductors, capacitors, diodes and the main switch have a negligible resistance.

The ZVT boost converter operates in nine different modes during a periodic switching cycle in steady state. The initial values of $I_{Lr1}(t_0)$, $I_{Lr2}(t_0)$, and $C_r(t_0)$ are reset to zero and $V_{Cs}(t_0) = V_o$ at the beginning of each cycle. The equivalent circuits of each mode are

shown in Figure 3.2 and the typical waveforms are illustrated in Figure 3.3. The equations that characterize each mode are established as follows:

Mode 1 *($t_0$–$t_1$)*: At t = $t_o$, the auxiliary switch $S_2$ is turned on with ZCS because of the inductor $L_{r1}$. The current flowing through $L_{r1}$ $L_{r2}$ and $C_r$ increases as the current is being diverted away from the main diode $D_1$. The mode ends at t = $t_1$ when the current flowing through $D_1$ is zero. The state equations for this mode are given in (3-1) to (3-4):

$$C_r \frac{d}{dt} v_{Cr(t)} = i_{Lr2(t)} - i_{Lr1(t)} \tag{3-1}$$

$$C_{s1} \frac{d}{dt} v_{Cs1(t)} = 0 \tag{3-2}$$

$$L_{r1} \frac{d}{dt} i_{Lr1(t)} = v_{Cr(t)} \tag{3-3}$$

$$L_{r2} \frac{d}{dt} i_{Lr2(t)} = V_0 - v_{Cr(t)} \tag{3-4}$$

The solutions to the above equations are given below in (3-5) to (3-8). The resonant frequency of this mode is represented by (3-9) and its equivalent inductance is described by (3-10).

$$v_{Cr}(t) = V_o \frac{L_{r1}}{L_{r1} + L_{r2}} (1 - \cos \omega_{eq} t) \tag{3-5}$$

$$v_{Cs1}(t) = V_o \tag{3-6}$$

$$i_{Lr1}(t) = V_o \frac{1}{L_{r1} + L_{r2}} (t - \frac{\sin \omega_{eq} t}{\omega_{eq}}) \tag{3-7}$$

$$i_{Lr2}(t) = V_o \frac{1}{L_{r2}(L_{r1} + L_{r2})} (L_{r2} t + \frac{L_{r1} \sin \omega_{eq} t}{\omega_{eq}}) \tag{3-8}$$

Where:

$$\omega_{eq} = \sqrt{\frac{1}{C_r L_{eq}}} \tag{3-9}$$

$$L_{eq} = \frac{L_{r1} L_{r2}}{L_{r1} + L_{r2}} \tag{3-10}$$

Mode 2 ($t_1$–$t_2$): At t = $t_1$, the capacitor $C_{s1}$ of the main switch begins to be discharged through the auxiliary circuit. This process involves $L_{r1}$, $L_{r2}$, $C_r$, $C_{s1}$ , $D_3$, $D_4$ and $S_2$. As a result, the current $i_{Lr1}(t)$, and voltage $V_{Cr}(t)$ continue to increase. $i_{Lr2}(t)$ reaches its maximum value and begins to decrease when $V_{Cs}(t)$ drops below $V_{Cr}(t)$, $C_{s1}$ is still being discharged until it is totally discharged at t= $t_2$, while the main switch body-diode begins to conduct. The state equations for this mode are given in (3-11) to (3-14):

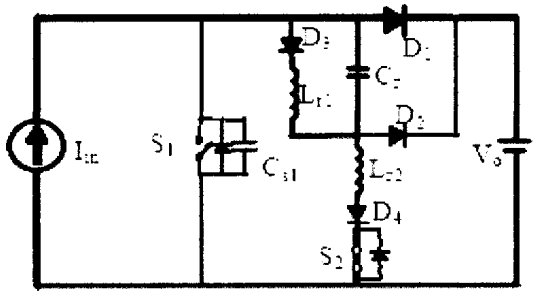

Mode 1 [$t_0$, $t_1$]

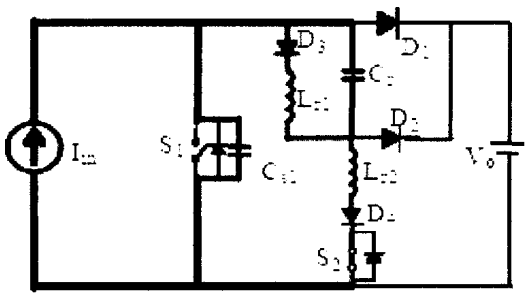

Mode 2 [$t_1$, $t_2$]

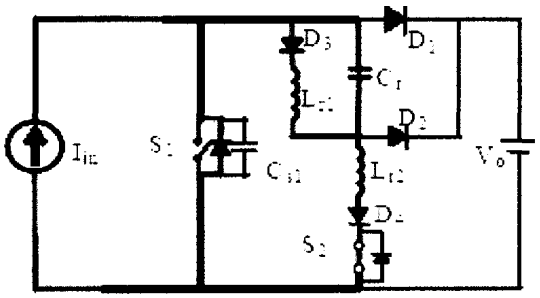

Mode 3 [$t_2$, $t_3$]

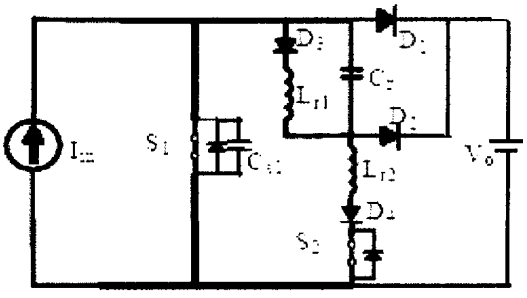

Mode 4 [$t_3$, $t_4$]

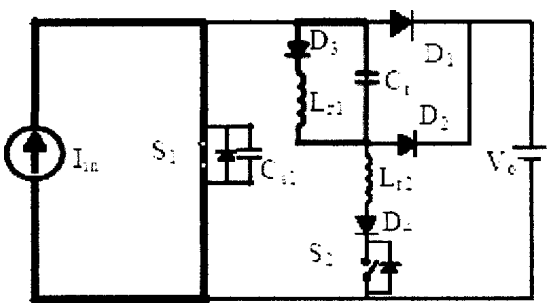

Mode 5 [$t_4$, $t_5$]

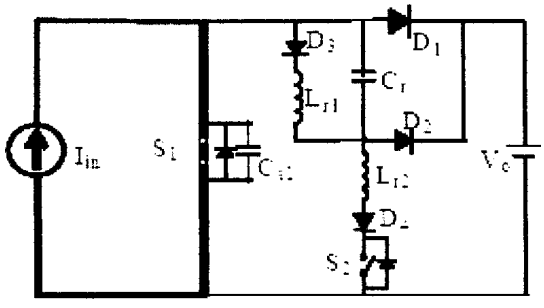

Mode 6 [$t_5$, $t_6$]

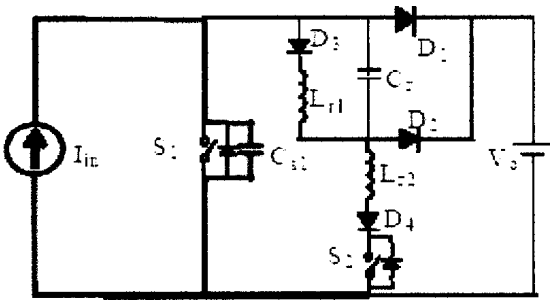

Mode 7 [$t_6$, $t_7$]

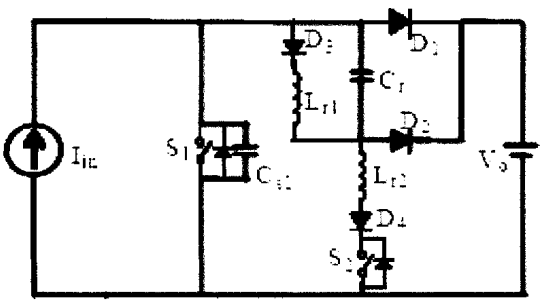

Mode 8 [$t_7$, $t_8$]

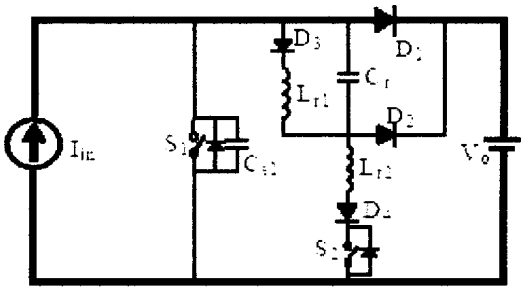

Mode 9 [$t_8$, $t_9$]

Figure 3.2. Operation modes of ZVT boos converter.

$$C_r \frac{d}{dt} v_{Cr(t)} = i_{Lr2(t)} - i_{Lr1(t)} \tag{3-11}$$

$$C_{s1} \frac{d}{dt} v_{Cs1(t)} = i_{Lr2} - I_o \tag{3-12}$$

$$L_{r1} \frac{d}{dt} i_{Lr1(t)} = v_{Cr(t)} \tag{3-13}$$

$$L_{r2} \frac{d}{dt} i_{Lr2(t)} = v_{Cs1(t)} - v_{Cr(t)} \tag{3-14}$$

The solutions to the above equations are given below in (3-15) to (3-18). This operation mode has two distinct resonant frequencies $\omega_x$ and $\omega_y$ represented in (3-19) and (3-20).

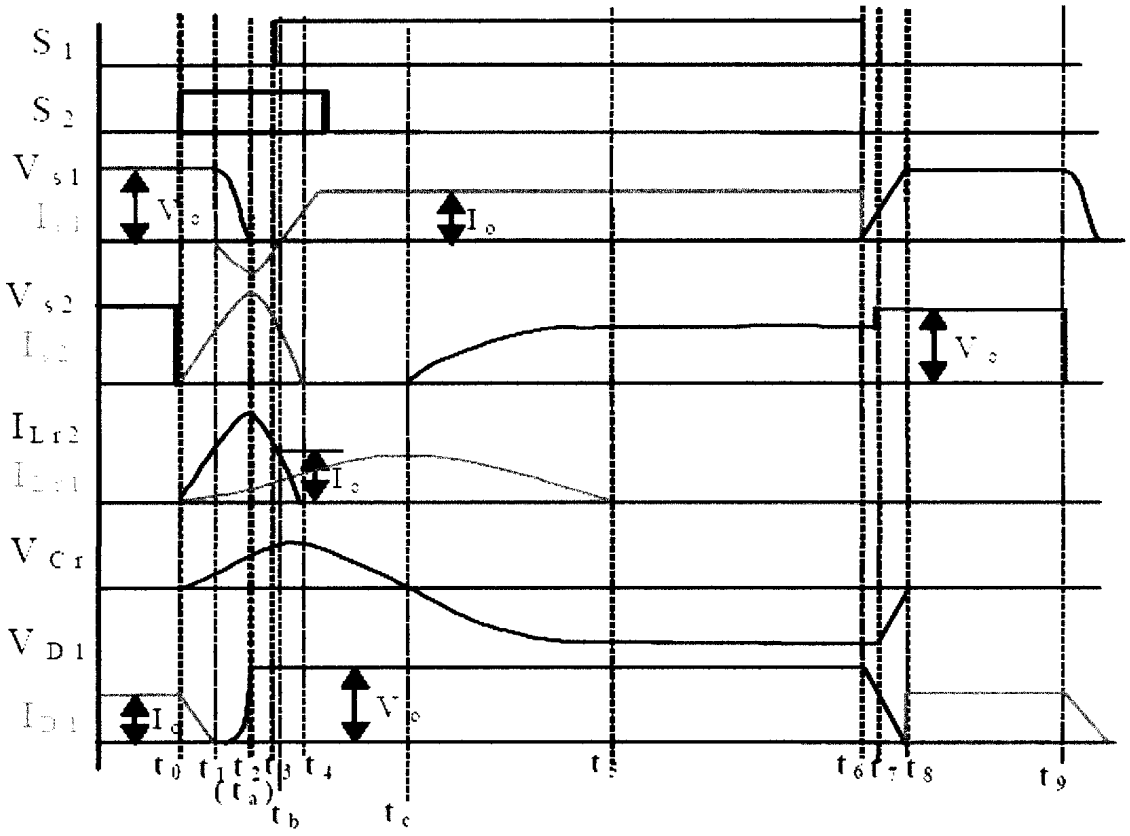


Figure 3.3. Typical switching waveforms.

$$v_{Cr}(t)=\left[V_{Cr}(t_1)\left(\frac{M_1}{C_{s1}L_{r2}\omega_x}-M_1\omega_x\right)+V_o\left(\frac{N_1}{C_{s1}L_{r2}\omega_x}-N_1\omega_x\right)\right]\cos\omega_x(t-t_1)$$

$$+\left[V_{Cr}(t_1)\left(\frac{M_2}{C_{s1}L_{r2}\omega_y}-M_2\omega_y\right)+V_o\left(\frac{N_2}{C_{s1}L_{r2}\omega_y}-N_2\omega_y\right)\right]\cos\omega_y(t-t_1)$$

$$+(I_{Lr1}(t_1)-I_o)P\left[\left(\frac{1}{\omega_x}-\omega_x L_{r2}\right)\sin\omega_x(t-t_1)-\left(\frac{1}{\omega_y}-\omega_y L_{r2}\right)\sin\omega_y(t-t_1)\right] \qquad (3\text{-}15)$$

$$v_{Cs}(t)=\frac{\frac{V_{Cr}(t_1)M_1}{L_{r2}\omega_x}+\frac{V_oN_1}{L_{r2}\omega_x}}{C_{s1}}\cos\omega_x(t-t_1)+\frac{\frac{V_{Cr}(t_1)M_2}{L_{r2}\omega_y}+\frac{V_oN_2}{L_{r2}\omega_y}}{C_{s1}}\cos\omega_y(t-t_1)$$

$$+\frac{(I_{Lr1}(t_1)-I_o)P}{C_{s1}\omega_x}\sin\omega_x(t-t_1)-\frac{(I_{Lr1}(t_1)-I_o)P}{C_{s1}\omega_y}\sin\omega_y(t-t_1)+V_o \tag{3-16}$$

$$i_{Lr1}(t)=\frac{V_{Cr}(t_1)(\frac{M_1}{C_{s1}L_{r2}\omega_x^2}-M_1)+V_o(\frac{N_1}{C_{s1}L_{r2}\omega_x^2}-N_1)}{L_{r1}}\sin\omega_x(t-t_1)$$

$$+\frac{V_{Cr}(t_1)(\frac{M_2}{C_{s1}L_{r2}\omega_y^2}-M_2)+V_o(\frac{N_2}{C_{s1}L_{r2}\omega_y^2}-N_2)}{L_{r1}}\sin\omega_y(t-t_1)$$

$$+\frac{(I_{Lr1}(t_1)-I_o)P}{L_{r1}}\left[(L_{r2}-\frac{1}{\omega_x^2})\cos\omega_x(t-t_1)-(L_{r2}-\frac{1}{\omega_y^2})\cos\omega_y(t-t_1)\right]$$

$$+\frac{V_o(t-t_1)}{L_{r1}}+I_{lr1}(t_1) \tag{3-17}$$

$$i_{Lr2}(t)=\frac{V_{Cr}(t_1)M_1+V_oN_1}{L_{r2}}\sin\omega_x(t-t_1)+\frac{V_{Cr}(t_1)M_2+V_oN_2}{L_{r2}}\sin\omega_y(t-t_1)$$

$$+(I_o-I_{Lr1}(t_1))P(\cos\omega_x(t-t_1)-\cos\omega_y(t-t_1))+I_o \tag{3-18}$$

Where:

$$\omega_x=\sqrt{\frac{(\omega_1^2+\omega_2^2+\omega_3^2)+\sqrt{(\omega_1^2+\omega_2^2+\omega_3^2)^2-4\omega_2^2\omega_3^2}}{2}} \tag{3-19}$$

$$\omega_y=\sqrt{\frac{(\omega_1^2+\omega_2^2+\omega_3^2)-\sqrt{(\omega_1^2+\omega_2^2+\omega_3^2)^2-4\omega_2^2\omega_3^2}}{2}} \tag{3-20}$$

$$\omega_1=\sqrt{\frac{1}{L_{r2}C_r}}\quad \omega_2=\sqrt{\frac{1}{L_{r2}C_{s1}}}\quad \omega_3=\sqrt{\frac{1}{L_{r1}C_r}}$$

$M_1$, $M_2$, $N_1$, $N_2$ and P are given as follows:

$$M_1 = \frac{-\sqrt{2}\omega_x}{-\omega_y^2+\omega_1^2+\omega_2^2+\omega_3^2} \qquad M_2 = \frac{-\sqrt{2}\omega_y}{-\omega_y^2+\omega_1^2+\omega_2^2+\omega_3^2}$$

$$N_1 = \frac{\omega_x(\omega_x^2-2\omega_1^2-2\omega_3^2)}{\sqrt{2}(-\omega_y^2+\omega_1^2+\omega_2^2+\omega_3^2)\omega_2^2} \qquad N_2 = \frac{\omega_y(\omega_y^2-2\omega_1^2-2\omega_3^2)}{\sqrt{2}(-\omega_y^2+\omega_1^2+\omega_2^2+\omega_3^2)\omega_2^2}$$

$$P = \frac{-\sqrt{2}\omega_1^2}{-\omega_y^2+\omega_1^2+\omega_2^2+\omega_3^2}$$

Mode 3 ($t_2$–$t_3$): At $t = t_2$, the body-diode of the main switch begins to conduct as $i_{Lr2}(t)$ is larger than $I_o$. Current $i_{Lr1}(t)$ and voltage $V_{Cr}(t)$ continue to increase. Some time during this mode, a resonant process involving the resonant branch of the auxiliary circuit begins and currents $i_{Cr}$ and $i_{Lr2}(t)$ start to decrease. It continues to do so until $t = t_3$, when the main switch $S_1$ can be turned on with ZVS. The state equations for this mode are given in (3-21) to (3-24).

$$C_r\frac{d}{dt}v_{Cr(t)} = i_{Lr2(t)} - i_{Lr1(t)} \tag{3-21}$$

$$C_{s1}\frac{d}{dt}v_{Cs1(t)} = 0 \tag{3-22}$$

$$L_{r1}\frac{d}{dt}i_{Lr1(t)} = v_{Cr(t)} \tag{3-23}$$

$$L_{r2}\frac{d}{dt}i_{Lr2(t)} = -v_{Cr(t)} \tag{3-24}$$

The solutions to the above equations are given below in (3-25) to (3-28). The resonant frequency in this mode is described by (3-29) and its equivalent inductance is given by (3-30)

$$v_{Cr}(t) = (I_{Lr2}(t_2) - I_{Lr1}(t_2))L_{eq}\omega_{eq}\sin\omega_{eq}(t-t_2) + V_{cr}(t_2)\cos\omega_{eq}(t-t_2) \quad (3\text{-}25)$$

$$v_{Cs1}(t) = 0 \quad (3\text{-}26)$$

$$i_{Lr1}(t) = \frac{(I_{Lr1}(t_2) - I_{Lr2}(t_2))L_{eq}}{Lr1}\cos\omega_{eq}(t-t_2) + \frac{V_{cr}(t_2)}{Lr1\omega_{eq}}\sin\omega_{eq}(t-t_2) + I_{Lr1}(t_2) - \frac{(I_{Lr1}(t_2) - I_{Lr2}(t_2))L_{eq}}{Lr1} \quad (3\text{-}27)$$

$$i_{Lr2}(t) = \frac{(I_{Lr2}(t_2) - I_{Lr1}(t_2))L_{eq}}{Lr2}\cos\omega_{eq}(t-t_2) - \frac{V_{cr}(t_2)}{Lr2\omega_{eq}}\sin\omega_{eq}(t-t_2) + I_{Lr2}(t_2) - \frac{(I_{Lr2}(t_2) - I_{Lr1}(t_2))L_{eq}}{Lr2} \quad (3\text{-}28)$$

Where:

$$\omega_{eq} = \sqrt{\frac{1}{C_r L_{eq}}} \quad (3\text{-}29)$$

$$L_{eq} = \frac{L_{r1}L_{r2}}{L_{r1} + L_{r2}} \quad (3\text{-}30)$$

Mode 4 ($t_3$–$t_4$): At $t = t_3$, the main switch $S_1$ is turned on at ZVS and the resonant process that began in Mode 3 continues. Current $i_{Lr1}(t)$ and voltage $V_{Cr}(t)$ continue to increase during Mode 4 and currents $i_{Cr}$ and $i_{Lr2}(t)$ continue to decrease until $t = t_4$. At $t = t_4$, $i_{Lr2}(t)$ becomes zero and $i_{Lr1}(t) = -i_{Cr}(t)$ as diode $D_4$ blocks any negative resonant current that would otherwise flow. The equations defining this mode are the same as those of

Mode 3 and the solutions are also similar, except different timing parameters. The equations and solutions are given by equations (3-31) to (3-40):

$$C_r \frac{d}{dt} v_{Cr(t)} = i_{Lr2(t)} - i_{Lr1(t)} \tag{3-31}$$

$$C_{s1} \frac{d}{dt} v_{Cs1(t)} = 0 \tag{3-32}$$

$$L_{r1} \frac{d}{dt} i_{Lr1(t)} = v_{Cr(t)} \tag{3-33}$$

$$L_{r2} \frac{d}{dt} i_{Lr2(t)} = - v_{Cr(t)} \tag{3-34}$$

Solutions:

$$v_{Cr}(t) = (I_{Lr2}(t_3) - I_{Lr1}(t_3)) L_{eq} \omega_{eq} \sin \omega_{eq}(t - t_3) + V_{cr}(t_3) \cos \omega_{eq}(t - t_3) \tag{3-35}$$

$$v_{Cs1}(t) = 0 \tag{3-36}$$

$$i_{Lr1}(t) = \frac{(I_{Lr1}(t_3) - I_{Lr2}(t_3)) L_{eq}}{Lr1} \cos \omega_{eq}(t - t_3) + \frac{V_{cr}(t_3)}{Lr1 \omega_{eq}} \sin \omega_{eq}(t - t_3) + I_{Lr1}(t_3) - \frac{(I_{Lr1}(t_3) - I_{Lr2}(t_3)) L_{eq}}{Lr1} \tag{3-37}$$

$$i_{Lr2}(t) = \frac{(I_{Lr2}(t_3) - I_{Lr1}(t_3)) L_{eq}}{Lr2} \cos \omega_{eq}(t - t_3) - \frac{V_{cr}(t_3)}{Lr2 \omega_{eq}} \sin \omega_{eq}(t - t_3) + I_{Lr2}(t_3) - \frac{(I_{Lr2}(t_3) - I_{Lr1}(t_3)) L_{eq}}{Lr2} \tag{3-38}$$

Where:

$$\omega_{eq} = \sqrt{\frac{1}{C_r L_{eq}}} \tag{3-39}$$

$$L_{eq} = \frac{L_{r1} L_{r2}}{L_{r1} + L_{r2}} \tag{3-40}$$

Mode 5 ($t_4$–$t_5$): During this mode, the auxiliary switch can be turned off with ZCS as $i_{Lr2}(t)$ is zero and $i_{Cr}+i_{Lr1}=0$. The current through the main switch is equal to $I_{in}$ and the energy from inductor $L_{r1}$ is transferred to $C_r$. This mode ends at $t=t_5$ when the current through $L_{r2}$ becomes zero and diode $D_3$ prevents the current from reversing direction. The state equations for this mode are given in (3-41) to (3-44)

$$C_r \frac{d}{dt} v_{Cr(t)} = - i_{Lr1(t)} \tag{3-41}$$

$$C_{s1} \frac{d}{dt} v_{Cs1(t)} = 0 \tag{3-42}$$

$$L_{r1} \frac{d}{dt} i_{Lr1(t)} = v_{Cr(t)} \tag{3-43}$$

$$L_{r2} \frac{d}{dt} i_{Lr2(t)} = 0 \tag{3-44}$$

The solutions to the above equations are given below in (3-45) to (3-48). The resonant frequency in this mode is represented by (3-49) and its equivalent inductance is given by (3-50)

$$v_{Cr}(t) = \frac{I_{Lr1}(t_4)}{C_r \omega} \sinh \omega(t - t_4) + V_{cr}(t_4) \cosh \omega(t - t_4) \tag{3-45}$$

$$v_{Cs1}(t) = 0 \tag{3-46}$$

$$i_{Lr1}(t) = I_{Lr1}(t_4)\cosh\omega(t-t_4) + V_{cr}(t_4)C_r\omega\cosh\omega(t-t_4) \quad (3\text{-}47)$$

$$i_{Lr2}(t) = 0 \quad (3\text{-}48)$$

Where:

$$\omega = \sqrt{\frac{1}{C_r L_{eq}}} \quad (3\text{-}49)$$

$$L_{eq} = L_{r1} \quad (3\text{-}50)$$

Mode 6 ($t_5$–$t_6$): During this mode, the converter operates in the same way as a standard PWM boost converter. $V_{Cr1}(t)$, $V_{Cr2}(t,)$ $i_{Lr1}(t)$ and $i_{Lr2}(t)$ are given in (3-51) to (3 54):

$$v_{Cr}(t) = V_{Cr}(t_5) \quad (3\text{-}51)$$

$$v_{Cs1}(t) = 0 \quad (3\text{-}52)$$

$$i_{Lr1}(t) = 0 \quad (3\text{-}53)$$

$$i_{Lr2}(t) = 0 \quad (3\text{-}54)$$

Mode 7 ($t_6$-$t_7$): At t = $t_6$, the main switch $S_1$ turns off with ZVS and capacitor $C_{s1}$ begins to be charged by $I_{in}$. This mode ends when the sum of $V_{Cs1}$ and $V_{Cr}$ equals Vo. $V_{Cr1}(t)$, $V_{Cr2}(t,)$ $i_{Lr1}(t)$ and $i_{Lr2}(t)$ are given in (3-55) to (3-58):

$$v_{Cr}(t) = V_{Cr}(t_6) \quad (3\text{-}55)$$

$$v_{Cs1}(t) = \frac{I_{in}}{C_{s1}}(t-t_6) \quad (3\text{-}56)$$

$$i_{Lr1}(t) = 0 \tag{3-57}$$

$$i_{Lr2}(t) = 0 \tag{3-58}$$

Mode 8 ($t_7$–$t_8$): At $t = t_7$, $D_2$ begins to conduct and $I_{in}$ charges both $C_{s1}$ and $C_r$. The voltage across $C_r$ drops and the voltage across $C_{s1}$ continue to rise. This mode ends at t= $t_8$ when$V_{Cs1}$ reaches $V_o$ and $V_{Cr}$ goes to zero. The resonant energy stored in $C_r$ is transferred into the output through $D_2$ during this mode. $V_{Cr}(t)$, $V_{Cs1}(t)$ $i_{Lr1}(t)$ and $i_{Lr2}(t)$ are given in (3-59) to (3-62):

$$v_{Cr}(t) = \frac{I_{in}}{C_{s1} + C_r}(t - t_7) + V_{Cr}(t_7) \tag{3-59}$$

$$v_{Cs1}(t) = \frac{I_{in}}{C_{s1} + C_r}(t - t_7) + V_{Cs1}(t_7) \tag{3-60}$$

$$i_{Lr1}(t) = 0 \tag{3-61}$$

$$i_{Lr2}(t) = 0 \tag{3-62}$$

Mode 9 ($t_8$–$t_9$): At $t = t_8$, $I_{in}$ starts flowing through $D_1$, and the converter operates like a standard PWM converter until the auxiliary switch is turned on at the start of the next switching cycle. $V_{Cr}(t)$, $V_{Cs}(t,)$ $i_{Lr1}(t)$ and $i_{Lr2}(t)$ are given in (3-63) to (3-66):

$$v_{Cr}(t) = 0 \tag{3-63}$$

$$v_{Cs1}(t) = 0 \tag{3-64}$$

$$i_{Lr1}(t) = 0 \tag{3-65}$$

$$i_{Lr2}(t) = 0 \tag{3-66}$$

The following results should be noted from the above description of the converter's operation:

(i) The main switch $S_1$ of the boost converter can be operated with a ZVS turn-on because the redirected current is able to flow through its body-diode just before it is to be turned on.

(ii) The main switch of the boost converter can operate with a ZVS turn-off since the capacitor $C_{s1}$ across it slows down the rate of voltage rise when the switch is turned off.

(iii) The auxiliary switch can operate with a ZCS turn-on because the inductors in the auxiliary circuit slow down the rate of current rise when the switch is turned on.

(iv) The auxiliary switch can operate with a ZCS turn-off because the current in the

# Chapter 4 Converter Design and Auxiliary Circuit Off-Tuning

## 4.1 Introduction

Based on the results of the mathematical analysis performed in the previous chapter, the steady-state characteristics and properties of the ZVT-PWM boost converter with the example dual auxiliary circuit are discussed in this chapter. A design procedure for the selection of the converter components is then presented and demonstrated with an example circuit. Finally, a variation of the example dual auxiliary circuit that results in less current circulating in the auxiliary circuit but more auxiliary switch turn-off losses is introduced.

## 4.2 Steady State Characteristics

In this section, the equations for each of the modes of operation of the converter presented in Chapter 3 are used to generate graphs of steady-state characteristic curves to evaluate the performance of the converter with respect to certain key parameter values. A MATLAB program is used to generate the graphs. The basic approach that the program takes is to look at a particular operating point (i.e., a set consisting of input voltage, output load, etc.), and go through each mode of converter operation from the first to the last, keeping track of parameters such as auxiliary circuit inductor currents and capacitor voltages shown in Figure 4.1. If the final value of a parameter after a switching cycle is

equal to its initial value, then the operating point is considered to be at steady state and other information such as peak current values can be determined. Graphs of steady-state characteristics can then be generated if the program repeats this process for a number of operating points.

Graphs of characteristic curves for the auxiliary switch voltage, auxiliary switch peak current, and main switch peak current in the converter can be used in the design of the ZVT-PWM boost converter as they show how the value of a critical component such as a particular inductor or a capacitor affects currents and voltages in the converter. Although the equations in Chapter 3 were derived for the case when the input to the converter is a DC source, they can also be used to determine worst case operating conditions for the converter when it is operating with an AC input source as an AC/DC converter. Graphs of steady-state characteristic curves are shown in Figures 4.2–4.4. The curves have been captured according to the specifications in Table 4.1.

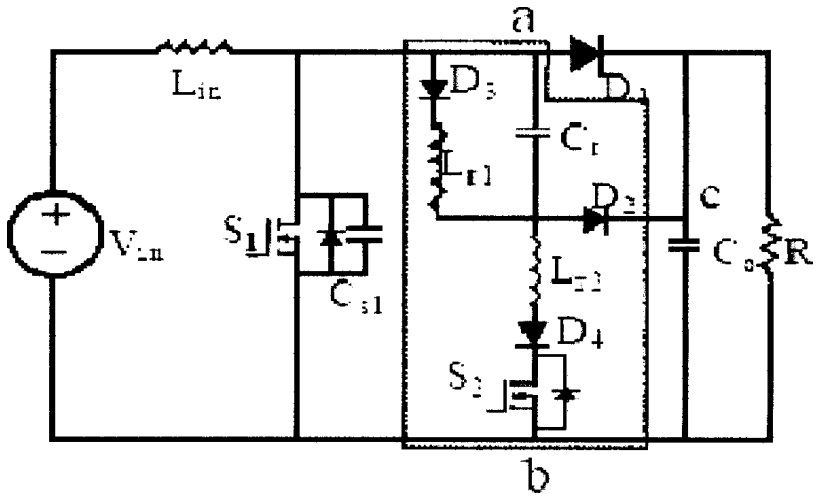


Figure 4.1. ZVT-PWM boost converter with dual auxiliary circuit.

Table 4.1 Converter Specifications for Characteristic Curves

| Input Voltage | Output Voltage | Output Power | Switching ($f_{sw}$) | Efficiency(η) |
|---|---|---|---|---|
| 100V DC | 400V DC | 500Watts | 100kHz | 95% |

The parameters in the graphs shown in Figures 4.2-4.4 have been normalized according to certain base values that are defined as follows:

$$V_B = V_o = 400\text{V} \tag{4-1}$$

$$I_B = \frac{P_{in}}{V_{in}} = \frac{P_0}{\eta * V_{in}} = 5.26\text{A} \tag{4-2}$$

$$Z_B = \frac{V_B}{I_B} = 76.05\Omega \tag{4-3}$$

$$T_B = \frac{1}{f_{SW}} = \frac{1}{100kH} = 10\mu\text{s} \tag{4-4}$$

The resonant impedance $Z_o$ is defined as:

$$Zo = \sqrt{\frac{L_{r2}}{C_{s1}}} \tag{4-5}$$

The parameter $K$ is defined as

$$K = \frac{C_r}{C_{s1}} \tag{4-6}$$

Where $C_{s1}$ is the capacitance across the main switch.

The characteristic curves shown in Figures 4.2–4.4 have been generated with different values of $K = C_r/C_{s1}$ and $Z_o/Z_B$ and with three different values of $L_{r1}$. Figure 4.2(a) shows the relationship between the peak values of the currents through inductors $L_{r1}$ and $L_{r2}$ and the normalized resonant impedance $Z_o/Z_B$. It can be seen that $i_{Lr1}$ (peak) increases and $i_{Lr2}$

(peak) decreases as $Z_o/Z_B$ increases or K decreases. This means that current $i_{Lr1}$ (peak) in non-resonant circuit increases and the current $i_{Lr2}$ (peak) in resonant circuit decreases if the value of $L_{r2}$ is increased and the capacitance of $C_s$ and $C_r$ are kept the same (increasing $Z_o$ and keeping K fixed) or if $C_r$ is decreased and $L_{r2}$ and $C_s$ are kept the same. Figures 4.2(a), 4.3(a) and 4.4(a) shows that the peak current through the inductor $L_{r2}$ is always larger than the peak current though $L_{r1}$ in a given range. The difference between them decreases as $Z_o$ increases. For the given range shown on the vertical axis, the current through $L_{r2}$ is always larger than $I_B$, the average current flowing in $L_{in}$.

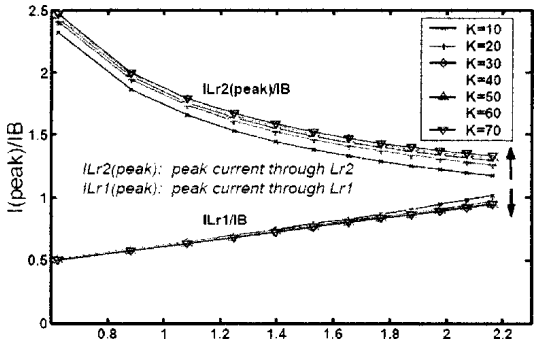


(a) Resonant Impedance $Z_o/Z_B$ ($L_{r1}$=25μH).

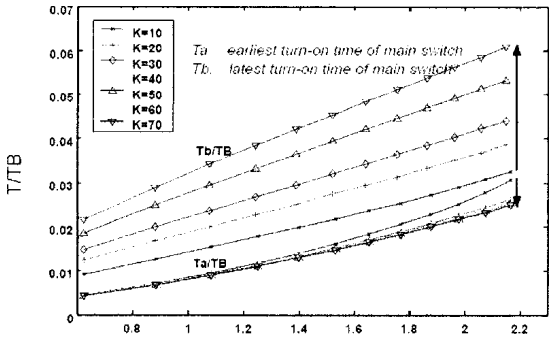


(b) Resonant Impedance $Z_o/Z_B$ ($L_{r1}$=25μH).

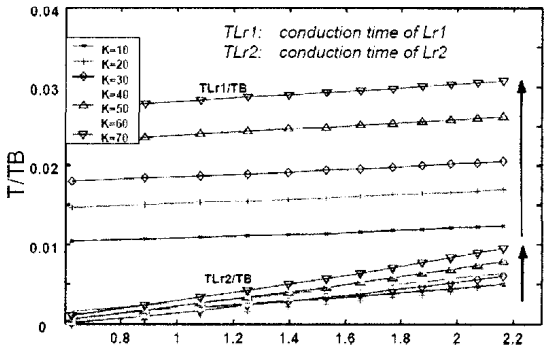


(c) Resonant Impedance $Z_o/Z_B$ ($L_{r1}$=25μH).

Figure 4.2. Characteristic curves for $L_{r1}$ =25 μH.

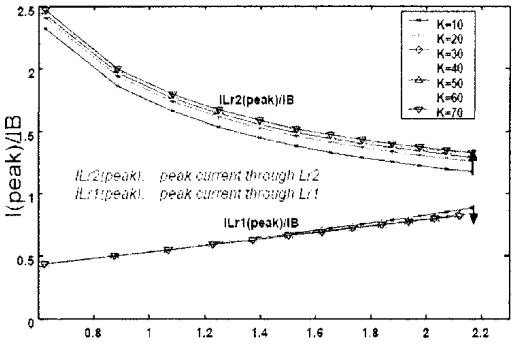


(a) Resonant Impedance $Z_o/Z_B$ ($L_{r1}$=33μH).

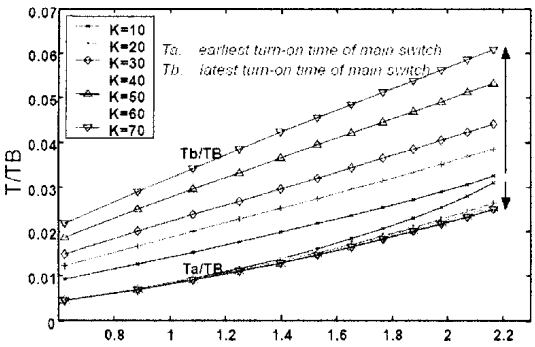


(b) Resonant Impedance $Z_o/Z_B$ ($L_{r1}$=33μH).

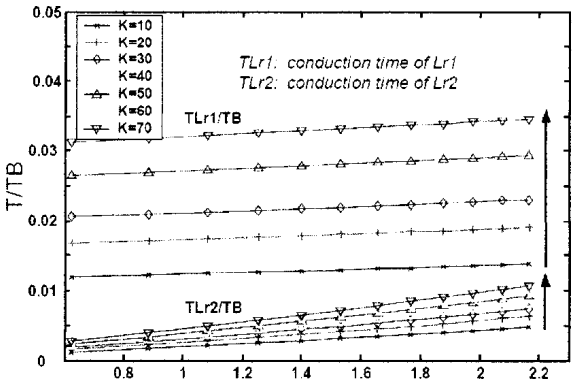


(c) Resonant Impedance $Z_o/Z_B$ ($L_{r1}$=33μH).

Figure 4.3. Characteristic curves for $L_{r1}$=33μH.

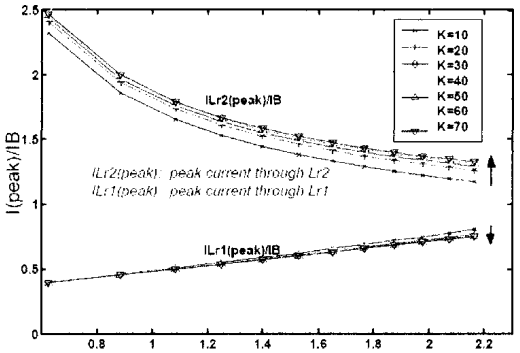


(a) Resonant Impedance $Z_o/Z_B$ ($L_{r1}$=40μH).

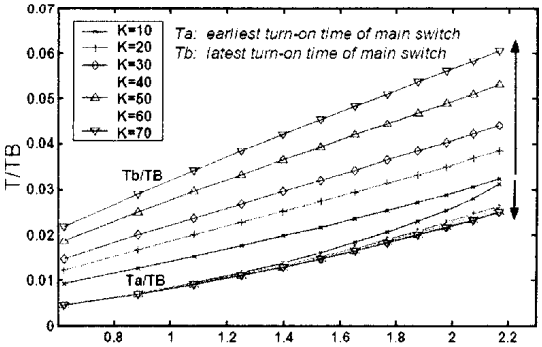


(b) Resonant Impedance $Z_o/Z_B$ ($L_{r1}$=40μH).

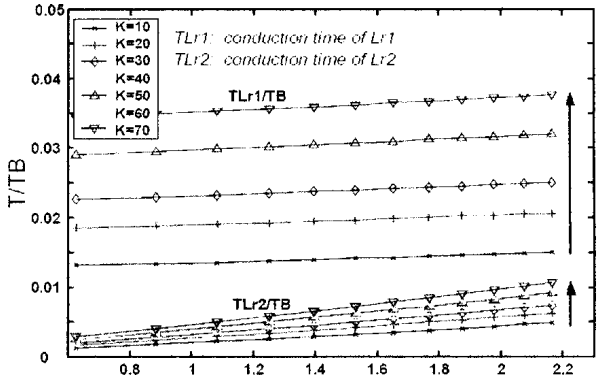


(c)Resonant Impedance $Z_o/Z_B$ ($L_{r1}$=40μH).

Figure 4.4. Characteristic curves for $L_{r1}$=40μH.

To ensure the ZVS turn-on of the main switch, $L_{r2}$ must be selected within a range of values that satisfy the condition $I_B < i_{Lr2}(peak)$, which enables the capacitor of the main switch to be discharged. At the same time, the current through inductor $L_{r1}$ should be as small as possible to reduce conduction losses in the auxiliary circuit. It can also be seen that K has a much smaller impact on the peak currents through both inductors than $Z_o/Z_B$.

Figures 4.2(b), 4.3(b) and 4.4(b) show the earliest and latest possible times that the main switch can be turned on with ZVS after the auxiliary switch has been turned on. In other words, the main switch will always have a ZVS turn-on as long as it turned on during a time interval between $T_a$ and $T_b$. In addition, it can be seen that the time interval $T_b$-$T_a$ does not significantly changes as $Z_o/Z_B$ increases but becomes significantly longer as $K$ increases. This indicates that the turn-on time interval of the main switch is mainly dependent on K.

Figures 4.2(c), 4.3(c) and 4.4(c) show the length of time that current is flowing through $L_{r1}$ and $L_{r2}$. It can be seen that this time increases for both $L_{r1}$ and $L_{r2}$ increases as $Z_o/Z_B$ and $K$ increases. It can be seen that $Z_o/Z_B$ mainly affects the time it takes for current to be

transferred from the boost diode to the auxiliary circuit when the auxiliary switch is turned on, and K mainly affects the resonant cycle of the resonant auxiliary circuit branch.

Figures 4.2-4.4 demonstrate that the $L_{r1}$ has little impact on the $i_{Lr1}$ (peak), whereas the $i_{Lr2}$ (peak) decreases as $L_{r1}$ increases. The turn on interval of main switch changes little as $L_{r1}$ increases. The time that current flows $L_{r1}$ becomes longer as $L_{r1}$ increases.

## 4.3 Converter Design Procedure

A procedure for the design of the ZVT-PWM boost converter shown in Figure 4.1 is presented in this section and is demonstrated with an example. For the example, the converter is to be designed according to the specification in Table 4.2. The design process is an iterative one and requires several revisions before the final design is completed. Only the final iteration will be shown in the example that follows. The design process consists of two parts, the design of the main power circuit and the design of the auxiliary circuit. The key objective in the design of the auxiliary circuit is to ensure that the auxiliary switch can turn off while it does not have current flowing through it, under the worst conditions. It should be noted that the similar design process is used for other boost converters with dual auxiliary circuits.

Table 4.2. Converter Specifications for Design Example

| Input Voltage | Output Voltage | Output Power | Switching $f_{sw}$ | Efficiency ($\eta$) |
|---|---|---|---|---|
| 100V–240VDC | 400V DC | 500 Watts | 100 kHz | 95% |

### 4.3.1 Main Power Circuit Design

1. Input Inductor $L_{in}$ Selection

For PWM boost converters, the value of input inductor is generally selected to limit the peak-to-peak ripple of the current flowing through the converter. A compromise must be made when selecting a value for $L_{in}$. If $L_{in}$ is too small, there will be an increase in main switch turn-off losses since the switch will turn off while it is conducting high peak current. If $L_{in}$ is too large, then the peak current will be small, but the physical size of the inductor will increase significantly and so too will the size and weight of the converter. A 20% peak-to-peak ripple to average current ratio of the input current is a compromise that is typically made and will also be made in this example. With this compromise, the boost converter is assumed to have a continuous current. From the given specifications, the maximum input current found by

$$I_{in} = \frac{Po}{\eta * V_{in}} = 5.26A \tag{4-7}$$

The peak-peak ripple to average ratio of the input current is taken to be 20% thus

$$\Delta I = 0.2 I_{in} = 1.05A \tag{4-8}$$

Rearranging the conversion ratio for the boost converter given in equation (1-2) to solve for the duty cycle D:

$$D = \frac{V_o - V_{in}}{V_o} = \frac{400 - 100}{400} = 0.75 \tag{4-9}$$

Consider

$$V_{Lin} = L_{in} \frac{di}{dt} \tag{4-10}$$

Where $V_{Lin}$ is the voltage across $L_{in}$ when $S_1$ on, dt = $D_{Tsw}$ is the time when the switch is on and *di* is the change in input current during that time, the value of $L_{in}$ can therefore be determined by:

$$L_{in} = \frac{V_{in}DT}{\Delta I} = \frac{100V * 0.75 * 10us}{1.05A} = 714\mu H \qquad (4\text{-}11)$$

The value of $V_{Lin}$ when $S_1$ is on is $V_{in}$. The minimum input voltage $V_{in}$ = 100V is used because this is when the maximum current flows in the converter.

## 2. Output Capacitor $C_o$ Selection

The minimum value of the capacitor can be determined by:

$$C_o > \frac{D}{Rf(\Delta V_o / V_o)} = \frac{0.75}{160 * 100000 * 0.01} = 469\mu F \qquad (4\text{-}12)$$

In practice, the filter capacitance value is often determined by the holdup requirements of the supply, not by ripple voltage considerations. This means that starting from an initial bus voltage, the capacitor must store enough energy to maintain the output above a specified minimum voltage, $V_{min}$, after the input voltage has been absent for a specified time, typically 20ms. Assuming that $V_{min}$ is 90% of $V_o$ and $T_h$ is the holdup time, during this holdup period, the energy transferred to the output is $E = P_o * T_h$, which is also equal to the energy discharged by the capacitor $C_o$ ($E = \frac{1}{2} C_o * (V_o^2 - V_{min}^2)$). $C_o$ is therefore determined by

$$C_o = \frac{2P_oT_h}{V_o^2 - V_{min}^2} = \frac{2 * 500 * 0.02}{400^2 - 360^2} = 658\mu F \qquad (4\text{-}13)$$

Considering the output voltage requirement, two 470μH/450V capacitors in parallel are selected.

## 3. Boost diode $D_1$ Selection

At minimum input voltage ($V_{in}$=100), the boost diode will handle the maximum peak input current that flows from the input through the diode when the switch is off. The maximum peak current through $D_1$ is therefore the same as the maximum peak current through the input inductor.

$$I_{peak} = I_{avg} + 0.5\Delta I = 5.26 + 0.5 * 1.05 = 5.79A \quad (4\text{-}14)$$

The maximum average current is determined to be

$$I = \frac{1-D}{1} * \frac{P_o}{\eta V_{in}} = (1-D) * \frac{P_o}{\eta V_o (1-D)} = \frac{500}{0.95 * 400} = 1.32A \quad (4\text{-}15)$$

so the diode selected must satisfy the peak current rating, the average current rating, which is 1.32A, and the voltage rating, which is 400V. In order to minimize problems of EMI and losses associated with the reverse-recovery characteristic of diodes (as described in Section 1.1.2 of this thesis) an ultra-fast diode should be selected. Taking this into consideration and the peak current, average current and peak voltage ratings into account, the International Rectifier HFA25TB60 with a recovery time $T_{rr}$ = 60ns is selected.

## 4. Main Switch MOSFET Selection

The MOSFET is the most widely used active semiconductor device in low-voltage (<1000V) high frequency (>100kHz) power converters because it can operate with simple drive requirements, fast switching speed, and fewer switching losses than other semiconductor devices. The main MOSFET in a ZVT-PWM converter must be able to withstand the full output voltage and be able to handle the RMS current through the

switch. The maximum voltage the MOSFET can handle is $V_o$ because it is clamped by the rectified diode $D_1$. The maximum rms (root-mean-square) value of the current through the MOSFET occurs when value of main diode $D_1$ is at its maximum, where D = 0.75 and $V_{in}$ = 100V DC

$$I_{rms} = \sqrt{\frac{(i_{\min}^2 + i_{\min} i_{\max} + i_{\max}^2)D}{3}} = 4.57A \qquad (4\text{-}16)$$

The MOSFET output capacitor $C_{oss}$ and its on-state resistance $R_{ds}(on)$ are important parameters to be considered when selecting the MOSFET because $C_{oss}$ affects switching losses and $R_{ds}(on)$ affects conduction losses. The smaller the value of $C_{oss}$, the smaller the size of components in the auxiliary circuit need be as less energy is needed to discharge the output capacitance of the main switch and to ensure its ZVS turn-on. The value of $C_{oss}$ should therefore be small as possible, but the smaller $C_{oss}$ is, the larger $R_{ds}(on)$ must be as there is an inverse relationship between the two in MOSFETs.

$R_{ds}(on)$ should be as small as possible to reduce conduction losses caused when the switch is on; a compromise between $C_{oss}$ and $R_{ds}(on)$ must be made. An International Rectifier IRFP460A has therefore been selected as a compromise device that can withstand the necessary peak voltage and RMS current stresses.

### 4.3.2 Auxiliary Circuit Design

The values of the auxiliary circuit components can be determined after the design of the main power circuit has been completed. This can be done using the graphs in Figures 4.2–4.4. Although these graphs and the components to be determined are specific to the converter in Figure 4.1, there are certain considerations that must be taken into account

regardless of the dual auxiliary circuit that is used. These considerations include the reverse-recovery time of the boost diode, when the auxiliary switch is to be turned on and for how long, and the amount of current circulating in the auxiliary circuit. The key objective in the design of the auxiliary circuit was to ensure that the auxiliary switch turns off while it does not have current flowing through it under the worst conditions. This can be done by designing the resonant branch of the auxiliary circuit so that it manages to divert all the current away from the switch before it is turned off.

For the converter shown in Figure 4.1, the values of components $L_{r1}$, $L_{r2}$ and $C_r$ can be determined in the following manner:

(1) Determine the minimum value of $L_{r2}$. The auxiliary circuit component values affect the rate at which current is transferred away from the diode. A slow, gradual rate of current transfer can significantly reduce the reverse recovery current of the main power circuit boost diode $D_1$. A good estimate for the quickest current transfer rate that will perform this task is to allow the current through the auxiliary circuit to ramp up to the boost diode current within three times the diode's specified reverse recovery time ($T_a>3t_{rr}$). The reverse recovery time of the device that was selected in Section 4.3.1.3 to be the boost diode is approximately 60 ns, so that Ta must at least 180 ns to satisfy the $T_a>3t_{rr}$ criterion. Fig. 4.5 shows an example of how to find the minimum value of $L_{r2}$ by looking at the characteristic curve of $L_{r1}$ = 33μH and K=10. $T_a$ is determined by

$$\frac{T_a}{T_b} = \frac{180ns}{10000ns} = 0.018 \qquad (4\text{-}17)$$

According to the curve, $Z_o$ is 1.65 when $T_a$ is 180 ns, therefore the minimum value of $L_{r2}$ is determined by:

$$\frac{Z_o}{Z_b} = \sqrt{\frac{L_{r2}}{C_s}} = 1.65 \qquad (4\text{-}18)$$

where $C_s$ is 480 pF, which is the output capacitance of the IRFP460A. The minimum value of $L_{r2}$ is therefore $L_{r2}$ = 7.55 μH. A value of 7.8μH is selected to guarantee the soft-switch turn-on with the main switch in a wider tolerance range.

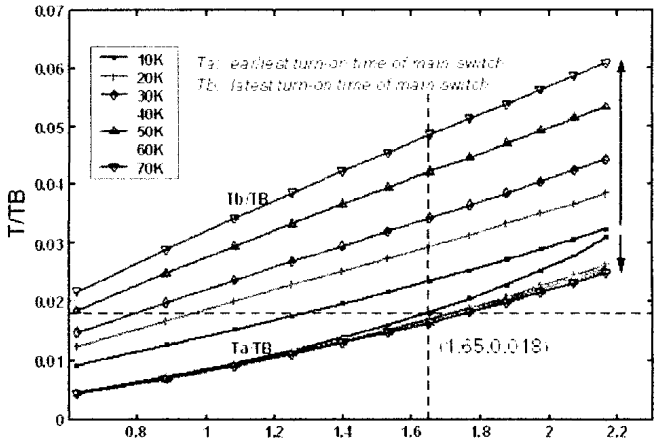


Fig 4.5. Characteristic curves for $L_{r1}$ = 33 μH and K=10 to be used in the selection of $L_{r2}$.

(2) Determine the value of $C_r$. In order to reduce the conduction loss, the time which current flows through $L_{r1}$ should be as short as possible. Between K=10 and K=70, K=10 provides the shortest conduction period for $L_{r1}$ and the auxiliary circuit; K =10 is therefore selected. The variable $C_r$ is determined by:

$$K = \frac{C_r}{C_s} = 10 \qquad (4\text{-}19)$$

thus

$$C_r = C_s * K = 480pF * 10 = 4.8nF \qquad (4\text{-}20)$$

A smaller $C_r$ (making K < 10) can be used in this case but the allowed turn-on time interval of the main switch will be narrower, making it more difficult to ensure that the main switch is turned on with ZVS. A 4.4nF ceramic capacitor is used in the prototype.

(3) Determine the value of $L_{r1}$. From Figs 4.2–4.4, it can be seen that when the value of $L_{r1}$ is smaller, which means a smaller size for the auxiliary circuit and larger $I_{peak}$. The value of $L_{r1}$, however, must be large enough to enable the current through $L_{r2}$ to reach zero. When this occurs, the current through $L_{r1}$ is equal to the current through $C_r$. If the value of $L_{r1}$ is too small such as $L_{r1}$ = 5 μH, the current through $L_{r2}$ is not able to become zero and the auxiliary switch has to be turned off hardly to divert the current. On the other hand, the value of $L_{r2}$ should not be too large so that the converter can operate with its maximum duty cycle without interference from the auxiliary circuit. There is an inverse relationship between the peak current that the auxiliary circuit must handle and the length of time that current flows in the auxiliary circuit. Both of these factors, however, affect auxiliary circuit conduction losses, but since increasing one by changing $L_{r1}$ decreases the other, the value of $L_{r1}$ therefore has little effect on the conduction losses. Values between 20μH and 35μH are suitable for this design example. $L_{r1}$ equal to 30μH is therefore chosen.

(4) Determine the ratings for the diodes of the auxiliary circuit. The currents through $D_2$, $D_3$ and $D_4$ are very small because the auxiliary circuit operates for about 5% of the switching cycle. The maximum peak current is the one through $D_4$ and $L_{r2}$ and it is designed to have a value of 1.2* $I_{peak}$, and $I_{peak}$ is the maximum peak current in the worst case through the input inductor $L_{in}$ and rectified diode $D_1$. This will allow the current through the auxiliary circuit to draw current from $D_1$ and discharge the body capacitor.

The maximum reverse voltage across $D_3$ is below 400 V and it occurs at the moment when the resonant capacitor $C_r$ is negatively charged by $L_{r1}$ and is clamped by $D_2$ as the main switch is still turned on.

The maximum reverse voltage across $D_4$ is also below 400 V and it occurs at the moment when the current through the auxiliary circuit is zero and the resonant capacitor $C_r$ is positively charged and is clamped by $D_1$ with the turn-on of the main switch. The maximum reverse voltage across $D_2$ is below 800 V and it occurs at the same moment when $D_4$ has its maximum reverse voltage. $D_3$ and $D_4$ can therefore be implemented with MUR420 devices and $D_2$ with a MUR460 device.

## 4.4 An Off-Tuned Dual Auxiliary Circuit

The dual auxiliary circuits above have the advantages of non-resonant and resonant auxiliary circuits without the disadvantages. The auxiliary switch can be turned off softly if the resonant branch diverts all of the current flowing through the switch before it is turned off. After this is done, there is current that circulates in the auxiliary circuit for some time before it dies down. Although this circulating current is less than that would appear in a resonant auxiliary circuit, it is still enough to create conduction losses.

The circulating current can be reduced if the resonant branch of the dual circuit is "off-tuned" so that the resonant branch diverts most, but not all the current in the auxiliary switch before it is turned off. In this case, the auxiliary switch has a hard turn-off, but with less current than it would if it was in a non-resonant auxiliary circuit. The fundamental principle behind the off-tuning of the resonant branch is to try to reduce conduction losses by reducing circulating current. Although auxiliary switch turn-off

losses increase, it is hoped that these losses are more than offset by the reduction in conduction losses.

Figure 4.6 shows a ZVT-PWM boost converter with an off-tuned variation of the dual auxiliary circuit in Chapter 3. This circuit has two parallel branches: a non-resonant branch consisting components: $L_{r1}$, $D_3$, $D_4$ and a resonant branch consisting of components: $L_{r2}$, $C_r$, $D_6$. The capacitor $C_r$ allows for an LC resonance between $L_{2r}$ and $C_r$ to return the inductor current to 0A. Diode $D_6$ allows the $C_r$ capacitor voltage to return to 0V every cycle by transferring the added energy to the output of each cycle, and preventing from accumulating. Additionally, diode $D_2$ is used to clamp the reverse-recovery spike cross the auxiliary switch $S_2$ when the inductor current returns to zero. The purpose of capacitor $C_r$* is to provide a path where the auxiliary switch current can be diverted to the load when the switch is turned off since there is a need to do so as the switch does not turn off softly. Energy from non-resonant branch $L_{r1}$ is transferred to $C_r$*, which is then eventually transferred to the output through the diode $D_5$ in a manner similar to that of the non-resonant circuit described in detail in Chapter 2 of this thesis.

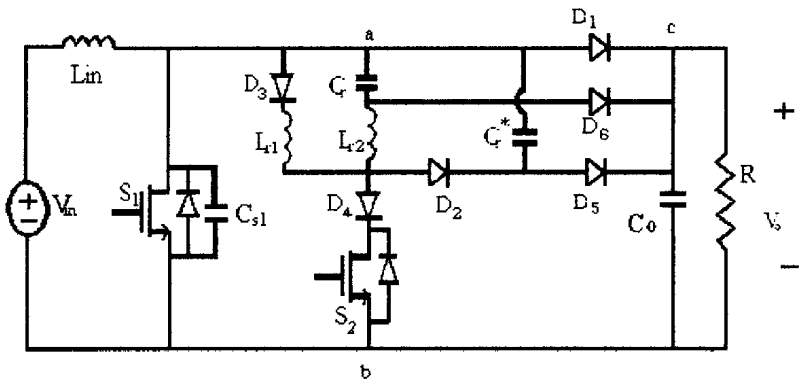


Figure 4.6. A ZVT-PWM boost converter with an off-tuned dual auxiliary circuit.

## 4.5 Conclusion

In this chapter, graphs of steady-state characteristics were generated using a MATLAB program and used as part of a design procedure that was demonstrated with an example. The procedure addressed the design of the main power circuit components and the auxiliary circuit components. The key objective in the design of the auxiliary circuit was to ensure that the auxiliary switch could be turned off with ZCS while it does not have current flowing through it, under the worst conditions. This was done by designing the resonant branch of the auxiliary circuit so that it manages to divert all of the current away from the switch before it is turned off.

Doing so, however, results in the appearance of a significant amount of current circulating in the auxiliary circuit. Although this circulating current is less than that found in a resonant auxiliary circuit, it is still enough to create conduction losses. In order to reduce these conduction losses, the concept of off-tuning the resonant branch of a dual circuit was introduced. The fundamental principle behind the off-tuning of the resonant branch is to try to reduce conduction losses by minimizing circulating current. Although auxiliary switch turn-off losses increase, it is hoped that these losses are more than offset by the reduction of conduction losses.

# Chapter 5 Experimental Results

## 5.1 Introduction

In this chapter, experimental results obtained from a prototype of 500W, 100 kHz ZVT-PWM boost converter are presented. The prototype was implemented with the dual auxiliary circuit discussed in Chapter 3, the off-tuned dual circuit presented in Chapter 4, and the original non-resonant and resonant circuits from which the dual circuit was derived. The efficiency of the converter operating with each of these four circuits is shown, experimental waveforms obtained with the converter operating with the off-tuned circuit are provided, and conclusions about the performance of all the circuits are made.

## 5.2 Experimental Results and Comparisons

Figure 5.1 shows a ZVT-PWM boost converter with a non-resonant auxiliary circuit, a resonant auxiliary circuit, a dual auxiliary circuit, and an off-tuned auxiliary circuit. Each experiment used the same base PWM boost circuitry, while the auxiliary circuit were applied separately to ensure that the layout topologies are identical for the power switches. Furthermore, each bench test used the same control circuitry and thermal management set-up. The converters were implemented with the component values shown in Table 5.1. The component values of the off-tuned circuit were obtained by slightly modifying those of the dual circuit.

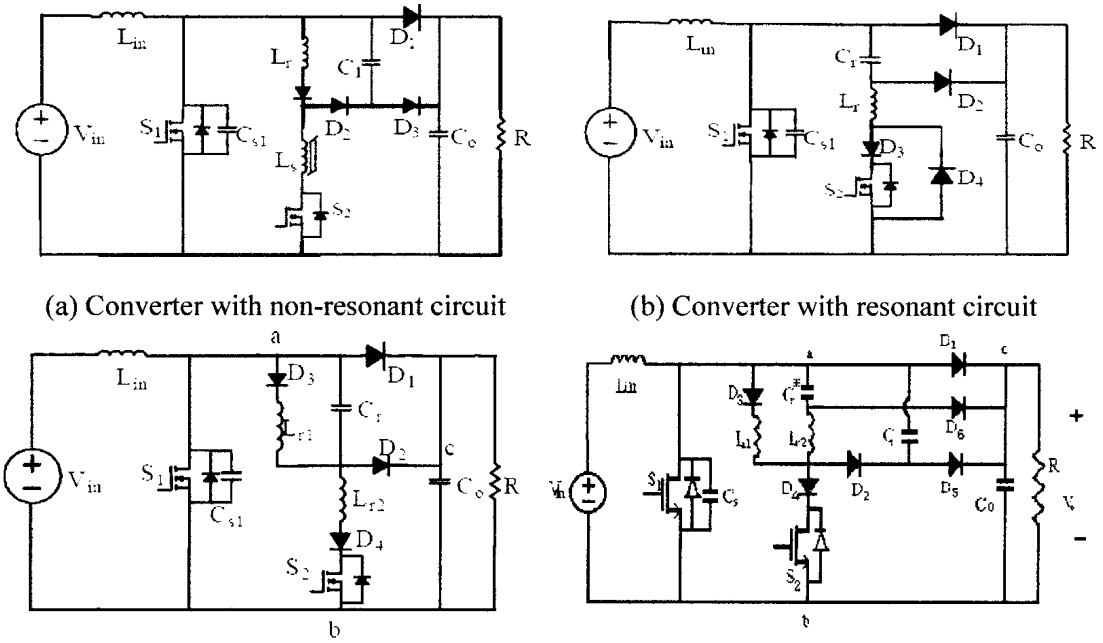

(a) Converter with non-resonant circuit

(b) Converter with resonant circuit

(c) Converter with dual circuit

(d) Converter with off-tuned circuit

Figure 5.1. ZVT-PWM Boost Converter with Various Auxiliary Circuits.

| Parameter | Off-tuned Auxiliary | Dual Auxiliary | Non resonant Auxiliary | Resonant Auxiliary |
|---|---|---|---|---|
| **Vi** | 108VDC | | | |
| **Vo** | 400VDC | 108VDC | 108VDC | 108VDC |
| **Po** | 5000 W | 400VDC | 400VDC | 400VDC |
| **$S_1$** | IRFP460 | 5000 W | 5000 W | 5000 W |
| **$S_2$** | IRF840 | IRFP460 | IRFP460 | IRFP460 |
| **$L_{in}$** | 330μH | IRF840 | IRF840 | IRF840 |
| **$C_o$** | 470μF | 330μH | 330μH | 330μH |
| **$L_{r1}$** | 18μH | 470μF | 470μF | 470μF |
| **$L_{r2}$** | 2.1μH | 30μH | 18μH | 5.8μH |
| **$C_{s1}$** | 2.2nF | 7.5μH | | |
| **$C_1$** | | 2.2nF | 2.2nF | 2.2nF |
| **$C_r$** | 10.5nF | | 1.2nF | |
| **$C_r$*** | 1.2nF | 4.4nF | | 1.2nF |
| **$D_1$** | HFA25TB60 | | | |
| **$D_2$** | MUR420 | HFA25TB60 | HFA25TB60 | HFA25TB60 |
| **$D_3$** | MUR420 | MUR420 | MUR420 | MUR420 |
| **$D_4$** | MUR460 | MUR420 | MUR420 | MUR420 |
| **$D_5$** | MUR420 | MUR460 | MUR460 | MUR460 |
| **$D_6$** | MUR420 | | | |

Table 5.1 Specifications and Components of the Prototype Circuit

Figure 5.2, shows the efficiency of the boost converters with the four different auxiliary circuits and without auxiliary circuit under fixed input voltage and fixed output power conditions respectively. The efficiency of each converter was measured from a 100 W to 500 W at 100 VDC input and 400 VDC output.

It can be seen from Figure 5.2 that the off-tuned dual circuit is the most efficient circuit. This is because this circuit has the advantages of the non-resonant and resonant circuits, but not the disadvantages, and it operates with less current circulating in it than the dual circuit.

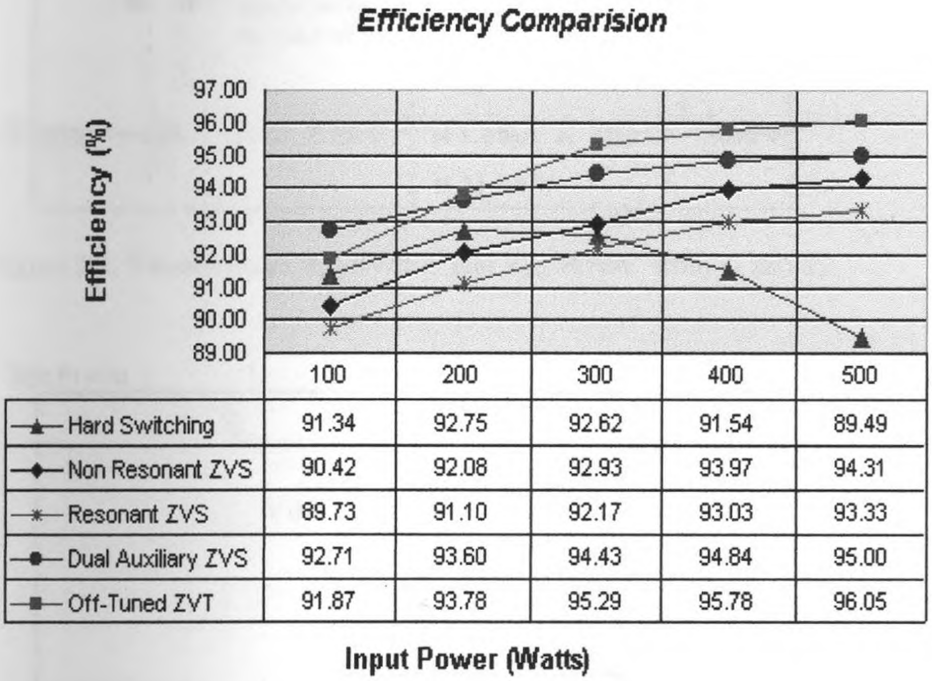


| | 100 | 200 | 300 | 400 | 500 |
|---|---|---|---|---|---|
| Hard Switching | 91.34 | 92.75 | 92.62 | 91.54 | 89.49 |
| Non Resonant ZVS | 90.42 | 92.08 | 92.93 | 93.97 | 94.31 |
| Resonant ZVS | 89.73 | 91.10 | 92.17 | 93.03 | 93.33 |
| Dual Auxiliary ZVS | 92.71 | 93.60 | 94.43 | 94.84 | 95.00 |
| Off-Tuned ZVT | 91.87 | 93.78 | 95.29 | 95.78 | 96.05 |

Figure 5.2 Experimental efficiency comparison at $V_{in}$ = 100 V.

Figure 5.3 shows typical voltage waveforms of the gating signals from the main switch $S_1$ and the auxiliary switch $S_2$ in the "off-tuned" experimental prototype. Figure

5.4 shows the drain to source voltage $V_{ds1}$ and the gate drive signal $V_{gs1}$ of the main switch $S_1$.

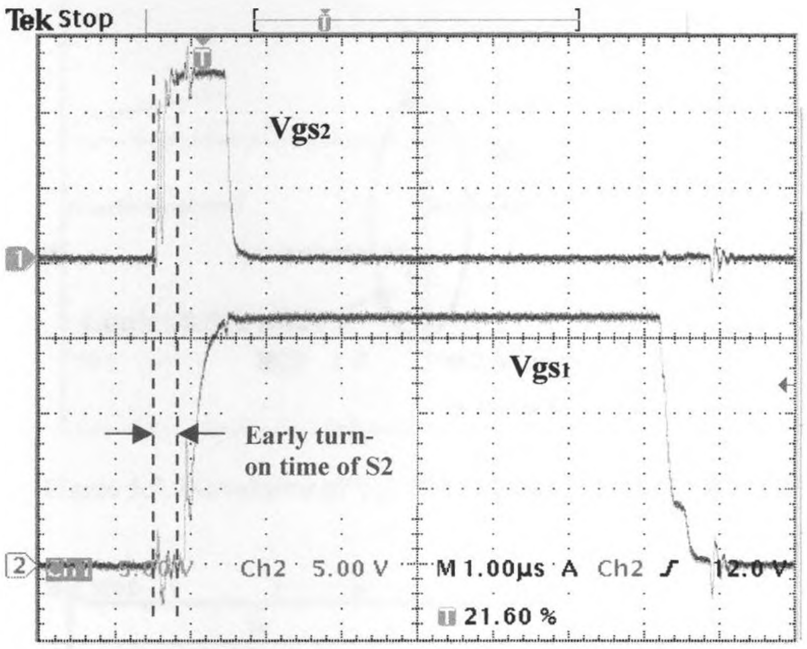


Figure 5.3. Waveforms of $V_{gs2}$ 5V/div and $V_{gs1}$ 5V/div from $S_2$ and $S_1$.

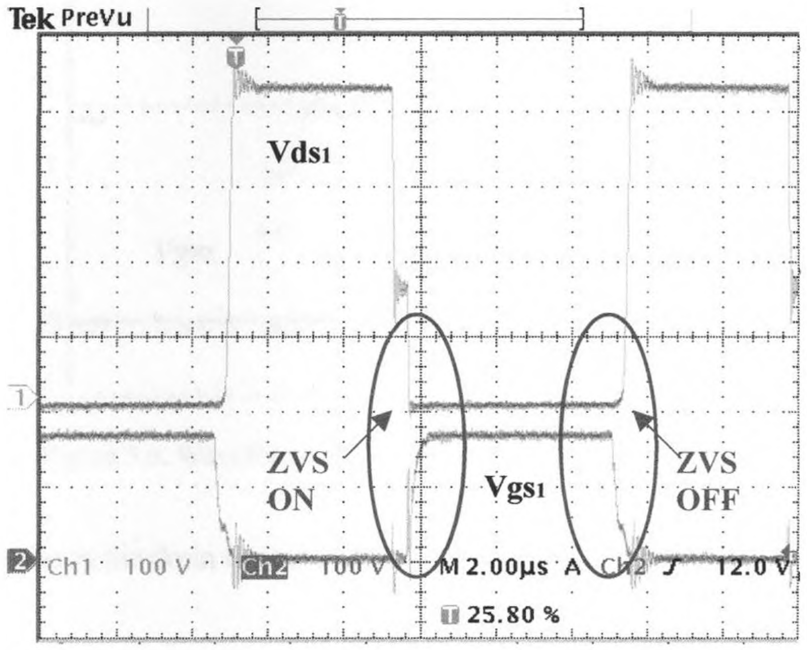


Figure 5.4. Waveforms of $V_{ds1}$ 100V/div and $V_{gs1}$ 10V/div from $S_1$.

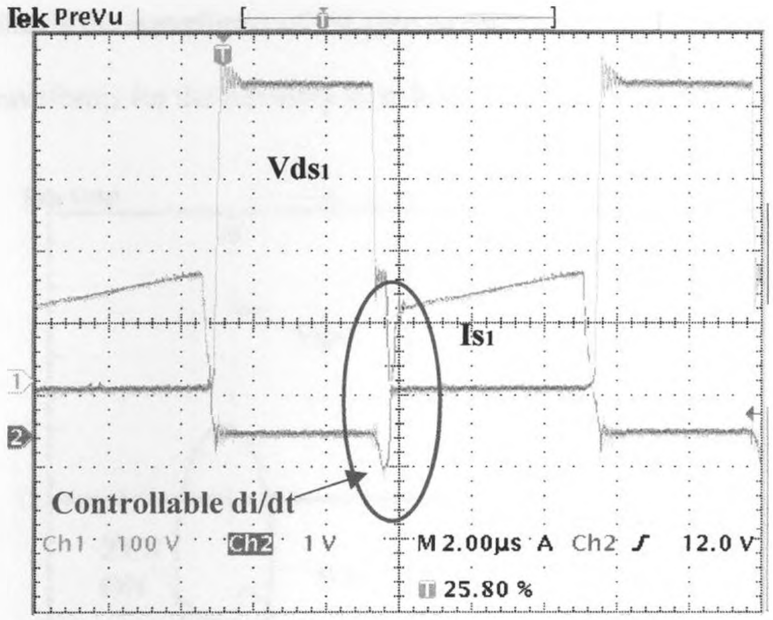


Figure 5.5. Waveforms of $V_{ds1}$ 100V/div and $I_{s1}$ 1A/div from $S_1$.

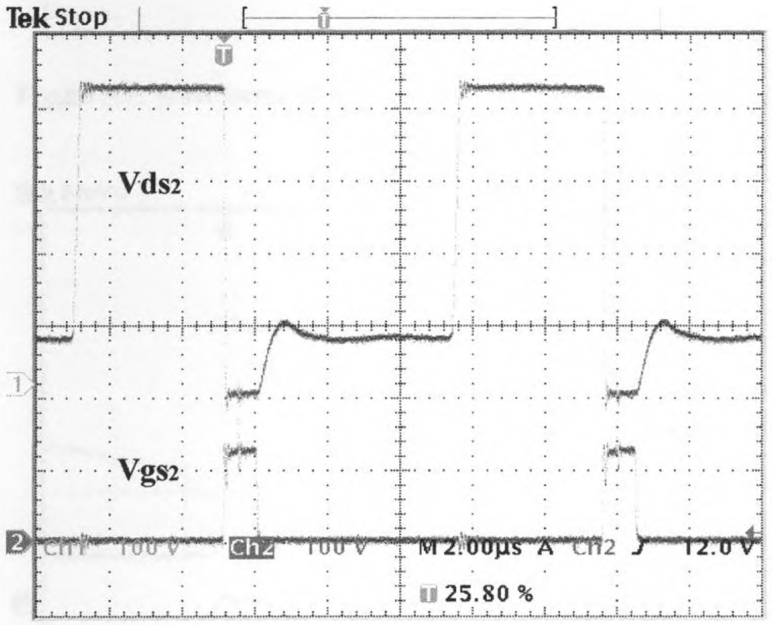


Figure 5.6. Waveforms of $V_{ds2}$ 100V/div and $V_{gs2}$ 10V/div from $S_2$.

Figure 5.5 shows the drain to source voltage $V_{ds1}$ and the current $I_{s1}$ of $S_1$.

Figure 5.6 shows the waveforms of the gate to source voltage $V_{gs2}$ and drain to source $V_{ds2}$ voltage waveforms for the auxiliary switch $S_2$.

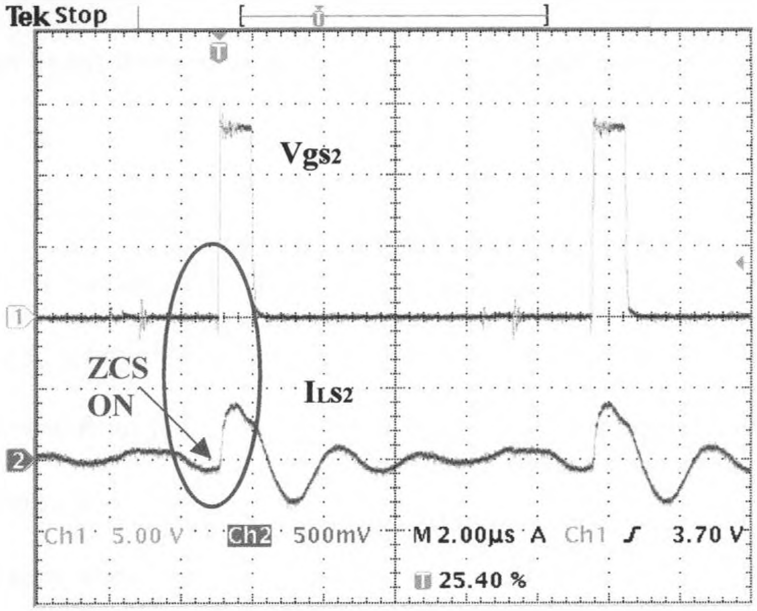


Figure 5.7. Waveforms of $V_{gs2}$ 5V/div and $I_{Lr1}$ 10A/div from $S_2$.

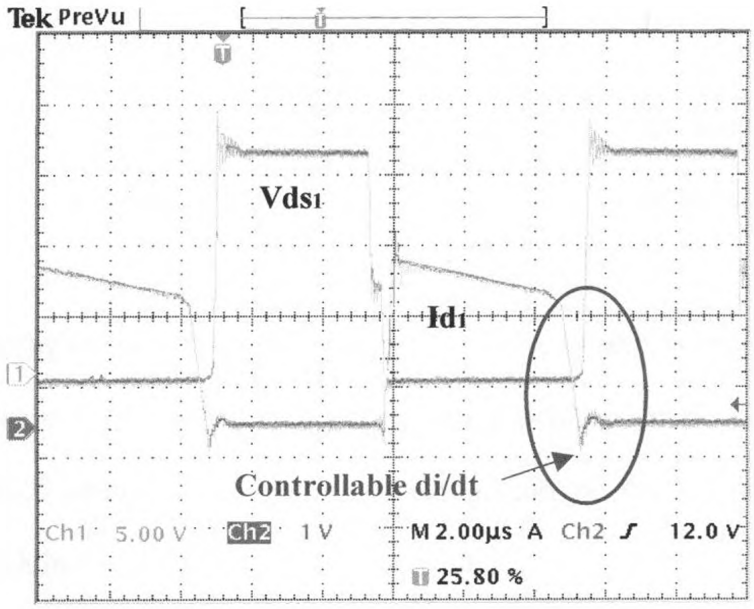


Figure 5.8. Waveforms of $V_{gs1}$ 5V/div and $I_{d1}$1A/div from $S_1$ and $D_1$.

Figure 5.7 shows the gate drive signal $V_{gs2}$ of $S_2$ and the inductor current $I_{Lr1}$ of the auxiliary circuit and Figure 5.8 shows the waveforms of the drain to source voltage $V_{gs1}$ of the main switch and the current $I_{d1}$ of main power diode $D_1$. The following observations can be made based on the waveforms presented in Figures 5.3 – 5.8:

(i) From the gate drive waveforms $V_{gs1}$ and $V_{gs2}$ in Figure 5.3, it can be seen that the auxiliary circuit is active for only a short duration (around 900ns) and only affects the operation of the converter when the main switch $S_1$ is being turned on. Moreover, the auxiliary switch $S_2$ is turned on around 400 ns earlier than the main switch $S_1$.

(ii) It can be seen from Figure 5.4 that the main switch $S_1$ turns on and off with zero-voltage switching (ZVS).

(iii) It can be seen from Figure 5.5 that the voltage across main switch $S_1$ drops to zero while the current through $S_1$ is negative. A negative current flowing through $S_1$ is an indication that current is flowing in the MOSFET switch's anti-parallel body diode after capacitor $C_{s1}$ has fully discharged. This confirms that $S_1$ can be turned on with zero-voltage switching (ZVS). In addition, the current flowing through $S_1$ does not show an over voltage spike and ringing, which would not be the case if a resonant auxiliary circuit were used.

(iv) The turning on and off of the auxiliary switch can be seen from Figure 5.6. It can be seen from Figure 5.7 that the auxiliary switch has a zero-current switching (ZCS) turn-on, but not a ZCS turn-off. The auxiliary switch has turn-on losses, but they are lower those for a switch in a non-resonant auxiliary circuit.

(v) It can be seen from Figure 5.8 that the negative current flowing in the main boost diode $D_1$ before it stops conducting is fairly small. Since this small negative current is

reverse-recovery current, the fact that it is small confirms that the auxiliary circuit can help minimize it.

## 5.3 Conclusion

Experimental results confirming the feasibility of a dual auxiliary circuit in a ZVT-PWM boost converter were presented. A prototype of 500W, 100 kHz DC-DC ZVT-PWM boost converter with input and output voltages of 100 VDC and 400 VDC respectively was built to compare the efficiency of the converter operating with a non-resonant auxiliary circuit, a resonant auxiliary circuit, a dual auxiliary circuit, and an off-tuned auxiliary circuit. It was shown that the converter with the off-tuned dual auxiliary circuit was the most efficient converter and that the dual auxiliary circuit concept was feasible. It was also shown that, in a ZVT-PWM boost converter with an off-tuned dual auxiliary circuit, the main converter switch can operate with soft-switching, that the auxiliary switch can operate with a ZCS turn-on but not a ZCS turn-off, and that the reverse-recovery current of the main boost diode can be significantly reduced.

# Chapter 6 Conclusion

## 6.1 Introduction

In this chapter, the major works of the thesis are summarized, the main contributions resulting from the thesis are stated, and suggestions for future work are given.

## 6.2 Summary

High frequency operation of pulse width modulated (PWM) boost converters allows for the reduction of the size and weight of their magnetic and filtering components; however, at high switching frequency, switching losses become significant and must be minimized. It has been accepted by power electronics researchers that the most efficient single-switch PWM converters with high frequency are zero-voltage transition (ZVT) PWM boost converters.

These converters contain an active auxiliary circuit that consists of an active switch and passive LC elements and that is not part of the main power circuit. The purpose of the auxiliary circuit is to help the main power switch, which is typically a MOSFET, to turn on with zero-voltage switching (ZVS). The auxiliary circuit is activated just before the main power switch is to be turned on and is active for only a fraction of the switching cycle, until the switching transition has been completed.

There have been many auxiliary circuits for ZVT-PWM boost converters that have been previously proposed by power electronics researchers. Most, if not all, of these

circuits are either one of two general types; an auxiliary circuit can be a non-resonant circuit or a resonant circuit. The auxiliary switch in a non-resonant circuit has considerable loss at turn-off as the flow of a significant amount of current through the switch is interrupted when the switch is turned off. The auxiliary switch in a resonant circuit has much lower turn-off loss, but the resonant circuit itself creates additional circulating current that increases conduction losses and the peak current stress of the main power switch.

The main objectives of this thesis were to propose a new type of auxiliary circuit that can be used in ZVT-PWM boost converters that combines the advantages of the non-resonant and resonant types of auxiliary circuits (reduce auxiliary switching losses without creating significant amounts of circulating current) and to study, characterize and examine the properties and characteristics of this new type of circuit through mathematical analysis and experimental work.

In the thesis, the general operation of a ZVT-PWM boost converter operating with a non-resonant and a resonant auxiliary circuit was reviewed. The new type of dual auxiliary circuit was then introduced and it was shown how a dual circuit can be derived from a non-resonant and a resonant circuit.

Several examples of the new type of dual circuit were presented and one of these was studied in detail. The operation of a ZVT-PWM boost converter with this example dual auxiliary circuit was explained and the key equations describing each mode of operation were derived. These equations were used to determine the steady-state characteristics of the converter and these, in turn, were used to develop a design procedure for the selection of the converter components.

A variation of the dual type of auxiliary circuit was then introduced and explained. In this variation, the resonant branch of the circuit was off-tune so that not all the current flowing in the auxiliary switch was diverted away from it before the switch is turned off. This variation had less circulating current than the original dual type but slightly more auxiliary switch turn-off losses.

Experimental results obtained from a prototype circuit of a 500 W, 100 kHz ZVT-PWM boost converter were presented. The prototype was implemented with the example dual auxiliary circuit, a variation of this circuit, and the original non-resonant and resonant circuits separately. The efficiency performance of the converters operating with each of these four circuits was shown

## 6.3 Conclusion

The following conclusions can be made based on the work done in this thesis:

(i) It is practical to develop a new dual auxiliary circuit by combining a non-resonant and a resonant auxiliary circuit, then eliminating redundant components.

(ii) It is feasible to design and develop a high frequency, single-switch PWM converter with the proposed dual auxiliary circuits.

(iii) The efficiency of a converter with a dual auxiliary circuit is greater than a converter with the non-resonant or resonant circuit from which the dual circuit was derived. Dual circuits do in fact have the advantages but not the disadvantages of non-resonant and resonant circuits.

(iv) Off-tuning the resonant branch of a dual auxiliary circuit results in greater converter efficiency, but at a higher cost since more components are needed. Although

the auxiliary switch in this circuit had greater turn-off losses than, the off-tuning of the resonant branch resulted in less circulating current being generated and this reduction in circulating current meant an overall increase in efficiency.

## 6.4 Contributions

The principal contributions of this thesis are as follows:

(i) A new type of auxiliary circuit that can be used in high frequency, single-switch PWM converters with the advantages, but not the disadvantages of non-resonant and resonant auxiliary circuits was presented.

(ii) Analysis on a circuit belonging to this new type was performed so that the properties and steady-state characteristics of the circuit were determined and an understanding of the circuit was developed.

(iii) The operation of an auxiliary circuit belonging to this new type was experimentally confirmed with results obtained from a prototype.

(iv) The off-tuned variation of the dual auxiliary circuit is one of the most efficient auxiliary circuits presently in existence as it has minimal losses.

## 6.5 Future Work

The following suggestions are made for future work:

(i) Future work can be done to confirm the feasibility of other dual circuits and to determine their relative efficiency.

(ii) The operation of an example dual auxiliary circuit was confirmed experimentally under a certain set of operating conditions (i.e., input voltage, output power). Future work can be done to confirm the operation of the circuit under other operating conditions.

(iii) It was shown how off-tuning the resonant branch of a dual auxiliary circuit results in increased converter efficiency. The off-tuning was performed by first designing a dual auxiliary circuit then doing the off-tuning. Future work can be done to develop a systematic method for determining the optimal amount of off-tuning that should be performed. Such work would require the use of optimization methods and modeling that were out the scope of the thesis.

(iv) Off-tuning the resonant branch resulted in greater efficiency, but also at greater cost as additional components were needed to snub the turn-off of the auxiliary switch, which was hard. Future work on minimizing the cost can be performed by examining whether a converter with an off-tuned dual auxiliary circuit can be simplified.

# References

[1] J. Bazinet and J. O'Connor, "Analysis and design of a zero-voltage transition power factor correction circuit," in *IEEE Appl. Power Elec. Conf. Rec.*, 1994, pp. 591–600.

[2] D. Zhang, D. Y. Chen, and F. C. Lee, "An experimental comparison of conducted EMI a hard switching circuit," in *IEEE Power Elec. Spec. Conf. Rec.*, 1996, pp.1992–1997.

[3] G. Moschopoulos, "Soft-switching power factor corrected converter topologies," Concordia Univ., Montr´eal, P.Q., Canada, 1996.

[4] L. H. Dixon, "High power factor switching pre-regulator design optimization," in *Unitrode Power Supply Design Seminar SEM700*, 1990.

[5] G. Hua and F. C. Lee, "Soft-Switching Techniques in PWM Converters," in *IEEE International Conference on Industrial Electronics, Control and Instrumentation,* 1993, pp.637–643.

[6] G. Hua, C. S. Keu, F. C. Lee "Novel Zero-Voltage Transition PWM Converters," in *IEEE Power Electronics Specialists Conference*, 1992, pp.55–60.

[7] R. Streit, D. Tollik, "A High Efficiency Telecom Rectifier Using A novel Soft-Switching Boost-Based Input Current Shaper," in *IEEE International Telecommunications Energy Conference*, 1991, pp.720–726.

[8] P. J. M. Menegas, S. L. Simonetti, J. L. F.Vieira, "Improving the Operation of ZVT DC-DC Converters," in *IEEE Power Electronics Specialists Conference*, 1999, Vol. 1, pp.293–297.

[9] T. W. Kim, H. S. Kim, H. W. Ahn, " An Improved ZVT PWM Boost Converter," in *IEEE Power Electronics Specialist Conference*, 2000, Vol. 2, pp.615–619.

[10] J. H. Kim, D. Y. Lee, H. S. Choi, B. H. Cho, "High Performance Boost PFP (Power Factor Pre-regulator) with an improved ZVT (Zero Voltage Transition) converter," in *IEEE Applied Power Electronics Conference*, 2001,Vol. 1, pp.337–342.

[11] L. C. de Freitas, D. F. da Cruz, V. J. Farias, "A Novel ZCS-ZVS-PMW DC-DC Buck Converter for High Power and High Switching Frequency: Analysis, Simulation and Experimental Results," in *IEEE Applied Power Electronics Conference*, 1993, pp.337–342.

[12] D. C. Martins, F. J. De Seixas, I. Barbi, J.A. Brilhante, "A Family of DC to DC PWM Converters Using a New ZVS Commutation Cell," in *IEEE Power Electronics Specialists Conference*, 1993, pp.524–530.

[13] N. P. Filho. V. J. Farias. L. C. deFreitas, "A Novel Family of DC-DC PWM Converters Using the Self-Resonance Principle," in *IEEE Power Electronics Specialists Conference*, 1994, pp.1385–1391.

[14] A. V. da Costa, C. H. G. Treviso, L. C. deFreitas, "A New ZCS-ZVS-PWM Boost Converter with unit Power Factor Operation," in *IEEE Applied Power Electronics Conference*, 1994, pp.404-410.

[15] J. P. Gegner, C. Q. Lee, "Zero-Voltage-Transition Converters Using a Simple Magnetic Feedback Technique," in *IEEE Power Electronics Specialists Conference*, 1994, pp.590–596.

[16] F. C. Lee, R. L. Lin, Y. Zhao, "Improved Soft-Switching ZVT converters with Active Snubber," in *IEEE Applied Power Electronics Conference*, 1998, Vol. 2, pp. 1063–1069.

[17] D. F. B. Gomes, R. S. F. Vincenzi, C. Bissochi Jr, J. B. Vieira Jr.,V. J. Farias, L. C. deFreitas, "A lossless Commutated Boost Converter as an Active Load for Burn-in Application," in *IEEE Applied Power Electronics Conference*, 2001,Vol. 2, pp.953–958.

[18] L. Yang, C. Q. Lee, "Analysis and Design of Boost Zero-Voltage-Transition PWM Converter," in *IEEE Applied Power Electronics Conference*, 1993, pp. 707–713.

[19] G. Moschopoulos, P. Jain, G. Joos, "A Novel Zero-Voltage Switched PWM Boost Converter," in *IEEE Power Electronics Specialists Conference*, 1995, Vol. 2, pp.694–700.

[20] K. M. Smith, K. M. Smedley, "A Comparison of Voltage-Mode Soft-Switching methods for PWM Converters," in *IEEE Transactions on Power Electronics*, 1997, Vol. 12, pp.376–386.

[21] G. Moschopoulos, P. Jain, G. Joos and Y. F. Liu, "Zero Voltage Switched PWM Boost Converter with An Energy Feedforward Auxiliary Circuit," in *IEEE Transactions on Power Electronics*, 1996,Vol. 1, pp.76–82.

[22] C. J Tseng, C. L. Chen, "Novel ZVT-PWM Converter With Active Snubbers," in *IEEE Transactions on Power Electronics*, 1998, Vol. 13, pp.861–869.

[23] N. Jain, P. Jain. G. Joos, " Analysis of a Zero Voltage Transition Boost Converter using a Soft Switching Auxiliary Circuit with Reduced Conduction Losses," in *IEE Power Electronics Specialists Conference*, 2001, Vol. 4, pp.1799–1804.

[24] N. Mohan, T.M. Undeland and W. P. Robins, "*Power Electronics* – Converters, Application and Design," John Wiley & Sons, NY. 1995.

[25] M. L. Martins, H. A. Grundling, H. Pinheiro, J. R. Pinheiro and H. L. Hey, "A ZVT PWM Boost Converter using Auxiliary Resonant Source," in *Seventeenth Annual* IEEE Applied Power Electronics Conference and Exposition, 2002, pp.1101–1107.

[26] L. H. Dixon, "High Power Factor Pre-regulators for Off-Line Power Supplies," Unitrode Power Supply Design Seminar SEM600. 1988 (Republished in subsequent Manuals).

[27] P. C. Todd, "UC3854 Controlled Power Factor Correction Circuit Design," Unitrode Application Note U-134.

[28] C. Zhou, R. B. Ridley and F. C. Lee, "Design and Analysis of an Active Unity Power Factor Correction Circuit," Annual Virginia Power Electronics Center Seminar Proceedings, September 1989.

[29] G. C. Hua, C. S. Leu, Y. M. Jiang and F. C.Lee, "Novel Zero Voltage Transition PWM Converters, IEEE Power Electronics Specialist Conference. 1992.

[30] J. G. Kassakian, M. F. Schlect, G. C. Verghese, "Principles of Power Electronics," Addison-Wesley, 1991.